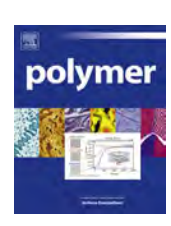


Contents lists available at ScienceDirect

Polymer

journal homepage: www.elsevier.com/locate/polymer



Dual-drug loaded Janus graphene oxide-based thermoresponsive nanoparticles for targeted therapy



Sepideh Khoee*, Mohammad Reza Karimi

Polymer Laboratory, School of Chemistry, College of Science, University of Tehran, PO Box 14155 6455, Tehran, Iran

ARTICLE INFO

Article history:
Received 18 September 2017
Received in revised form
5 March 2018
Accepted 12 March 2018
Available online 13 March 2018

Keywords:
Graphene oxide
Janus nanoparticles
Microemulsion
Dual-drug delivery
Thermoresponsive polymer

ABSTRACT

Graphene oxide (GO) is extensively recognized as an effective material in a variety of fields and specifically for various biomedical applications. However, the modification of each side of a GO sheet, needed for preparation of heterogeneous nanoparticles, is yet hypothetical and unclear. Here, we have developed a new strategy for the synthesis of two-faced GOs by simultaneous anchoring of different polymers with different hydro-affinity via Pickering emulsion (two-phase media). Alkynyl-modified GO was prepared for unsymmetrically attaching azidated-poly(£-caprolactone) (PCL) and (N-iso-propylacrylamide-co-acrylamide-co-allylamine) terpolymer to the surface of GO through click reaction. During this reaction, a thermoresponsive nanoparticles with specific morphology, known as "Janus" nanostructure, will be produced. PCL/terpolymer homostructure was also fabricated via solution (one-phase) reaction, where two types of polymers were grafted on the both surfaces of GO disorderly, named "mixed" nanoparticles. In the following, drug loaded nanocarriers were synthesized by simultaneously using quercetin and 5-FU as hydrophobic and hydrophilic drugs. The bioapplicability of these nanoparticles were evaluated by comparison of their in vitro release profiles and cell cytotoxicity at two temperatures of 37 and 40 °C.

© 2018 Elsevier Ltd. All rights reserved.

1. Introduction

Through utilizing the unique capabilities of nanotechnology, smart nanocarriers have been introduced which can overcome many drawbacks of traditional drug delivery systems through improvements in drug release properties in targeted delivery sites to reduce side effects in other regions [1]. Such side effects can be fatal in the case of cancer chemotherapy. In addition, while chemotherapeutic agents can effectively treat cancerous cells, repeating the single drug treatment may lead to chemotherapeutic drug resistance [2]. To address such issues, combination therapy has been used in many clinical trials as a promising approach for cancer treatment. Through combination therapy, two or more therapeutic components are simultaneously introduced into the body. Codelivery of different chemotherapeutics through dual drug delivery systems, as an example, aim to maximize the efficacy of therapy [1-4]. Due to the synergistic effects of different therapeutics and lowered levels for the administration of total dosage of these cytotoxic agents, such combinatory methods have become the most favored therapeutic modality to overcome side effects caused by high doses of single drugs [5]. Combination of chemotherapeutics and anti-oxidants have been reported to be effective for different cancer therapies [6], 5-fluorouracil and quercetin have shown to exhibit synergistic effects in colorectal and pancreatic cancers [1,7]. Finding carriers with proper load, and release properties are then of major concern. Janus particles, named after the mythological Roman god of gates, have been recently shown to be applicable in biomedical and drug delivery systems [8–11]. Such nanoparticles are generally made up of two different hemispheres with different chemistry and physical properties where they can play at least two different simultaneous roles of targeting and stimuli-based release for different payloads with different hydroaffinities [12].

Among the currently available synthetic approaches, Pickering emulsion strategy has proven to be successful in the synthesis of Janus particles. Pickering emulsion provides suitable conditions for the conjugation of hydrophobic and hydrophilic components solved in water or oil phases through the stabilizing effect by bringing solid nanoparticles at a vast interface between two liquid phases. On the other hand, graphene oxide (GO) is considered as an

^{*} Corresponding author. E-mail address: khoee@khayam.ut.ac.ir (S. Khoee).

appropriate platform for biodevice because of its highly efficient properties like biocompatibility, biodegradablility, biosensing, bioimaging and photo-thermal therapy [13,14]. Having multiple oxygen containing functional groups both at the surface and the edges can provide opportunity for graphene layers to be dispersed in both aqueous and polar organic phases [4]. Existence of such functional groups can also be used for chemical reactions to achieve permanent stabilization for long-term usage.

Previous attempts toward preparation of Janus GO mainly involved electrostatic assembly [15] and functionalization of large scale materials with different hydro-affinity functional groups in different sides and Pickering emulsion [16,17]. As it has unique amphiphilic structure, solid stabilization of foams and emulsions is considered as one of the most outstanding duties of Janus graphene oxide [18,19]. Yang et al. fabricated Janus GO nanosheets by using cationic polystyrene microspheres as micro-template and electrostatic assembling of GO nanosheets on their surface. Anchoring hydrophilic poly(2-(dimethylamino)ethyl methacrylate) chains on the other side can make GO-based Janus nanoparticles [15]. To prepare Janus GO with different hydro-affinity properties, millimeter-scale reduced GO sponges were synthesized by freeze drying (Tajhizat Sazan Pishtaz Co, Iran), and their wettability was controlled by fluorine (hydrophobic in air) or oxygen (hydrophilic in air) functionalizations [16]. Wu et al. prepared janus GO nanosheet through protecting one side of GO via wax-in-water Pickering emulsion method and grafting the free surface of the GO with epoxy groups. Janus GO, compared with symmetrically modified GO, shows potent stabilization in Pickering emulsion method [17].

Of the various significant research activities on GO chemistry that have been conducted, nearly no work to date has been focused on the simultaneous functionalization of graphene oxide using two hydrophobic and hydrophilic polymers via Pickering emulsion method. And between some few research articles about preparation of Janus GO, no one deals with practical applications of dual drugs delivery systems. In the present study, we demonstrate the synthesis of a new Janus graphene oxide nanoparticle, via covalently attaching different types of polymers on its two faces simultaneously, as an amphiphilic nanovehicle for combinatorial drug delivery approach. Our strategy in fabrication of this nanocarrier is based on the utilization of poly(N-isopropylacrylamideco-acrylamide-co-allylamine) terpolymer as the thermo-sensitive hydrophilic component and poly(ε-caprolactone) as the hydrophobic one. Graphene oxide was symmetrically decorated with alkynylated groups and the prepared pre-polymers were covalently attached to the surface of nano graphene oxide (NGO) through click reaction via two methods. Janus nanoparticles were synthesized via oil in water Pickering emulsion and "mixed" nanoparticle was obtained through a homogeneous solution. The procedure was followed by simultaneously or individually loading of quercetin and 5-FU as respective hydrophobic and hydrophilic drugs to investigate the possibility of using these particles in cancer combination therapy. In-vitro release profiles of 5-FU and quercetin were observed in phosphate buffer solutions at two temperatures, 37 and $40 \,^{\circ}\text{C}$ (pH = 7.4), to investigate the stimuli-responsiveness of the particles.

2. Experimental

2.1. Materials

Graphite flakes, potassium permanganate (KMnO₄), phosphoric acid (H₃PO₄), *N*,*N*-dicyclohexylcarbodiimide (DCC), 4-dimethylaminopyridine (DMAP), sodium azide (NaN₃), copper bromide (CuBr), azobisisobutyronitrile (AIBN), copper(II) sulfate pentahydrate and propargyl amine were obtained from Sigma-

Aldrich. ε -Caprolactone, N-isopropylacrylamide (NIPAAm), acrylamide (AAm), allylamine (AA), pentamethyldiethylene triamine (PMDETA), ascorbic acid, anhydrous magnesium sulfate, epichlorohydrin, sodium bicarbonate, tetra-n-butylammonium bromide (TBAB), dichloromethane (DCM), diethyl ether, N,N-dimethylformamide (DMF), sulfuric acid (H_2SO_4), hydrochloric acid (HCl), hydrogen peroxide (H_2O_2), 1,4-dioxane, and stannous octoate (H_2O_2) were all purchased from Merck Chemical Co. Triethylamine (TEA) was obtained from Fluka. All reagents and solvents were of analytical grade and used without any purification.

2.2. Preparation of nanoparticles

2.2.1. Azidation of epichlorohydrin

Azidated epichlorohydrin (AE) was synthesized according to the procedure described as previously reported [20]. Briefly, 5 g sodium azide (77 mmol) was dissolved in 15 mL deionized water, containing tetrabutylammonium bromide (0.16 g, 0.5 mmol) as a phase transfer catalyst, in a round-bottom flask followed by the dropwise addition of 7.11 g epichlorohydrin (6 mL, 77 mmol). Since the reaction products are highly photosensitive, reaction vessels were covered by aluminum foil and the mixture was allowed to proceed at room temperature for about 16 h. 20 mL dichloromethane was then added to the reaction mixture and non-aqueous layer was separated using a separating funnel. The organic layer was dried over anhydrous magnesium sulfate and its solvent was evaporated under reduced pressure by rotatory evaporator to yield the azidated epichlorohydrin with 72% yield.

2.2.2. Synthesis of poly(ε -caprolactone) with AE initiator

5 mL ε -caprolactone (45 mmol), 5 mL DMF and 675 mg AE (5 mmol) were poured into a three-necked round-bottom flask and purged with dried nitrogen. The mixture was heated to 80 °C and a catalytic amount of Sn(Oct)₂ was added to the reaction medium. The reaction temperature was raised up to 120 °C and kept constant at this temperature for 24 h. The crude product was precipitated in cold water and dried in a vacuum oven at 40 °C for 24 h to produce azide-terminated poly(ε -caprolactone) 73.2% yield.

2.2.3. Synthesis of poly(N-isopropylacrylamide-co-acrylamide-co-allylamine) poly(NIPAAm-co-AAm-co-AA), a thermo-sensitive polymer

Poly(NIPAAm-co-AAm-co-AA) (terpolymer) was prepared *via* random radical polymerization [21]. Briefly, 0.518 g (5 mmol) NIPAAm, 0.016 g (0.22 mmol) AAm, 0.022 mL (0.29 mmol) AA and 5 mL of dioxane were added into a three-necked round-bottom flask and let to stir for 30 min, under continuous nitrogen purging. 0.01 g AIBN was added to the mixture and the reaction temperature was adjusted to 60 °C using an oil bath and the system was stirred at this temperature for 24 h under nitrogen atmosphere. The resulting polymers were re-precipitated into cold diethyl ether and then dried under vacuum to obtain terpolymer with 77% yield.

2.2.4. Functionalized poly(NIPAAm-co-AAm-co-AA) by azide groups

Terpolymer (1.5 g) was dissolved in 1,4-dioxane, in a threenecked round-bottom flask, at room temperature and purged with nitrogen gas. 2 mL triethylamine (2.75 g) was added slowly to the above mixture and followed by dropwise addition of freshlyprepared azidated epichlorohydrin (3.5 g). The reaction solution was then stirred at 50 °C for 48 h. The reaction mixture was poured into cold diethyl ether, filtered and then dried under vacuum to yield crude azidated terpolymer. In order to further purify, the product was re-dissolved in 1,4-dioxane and re-precipitated in cold diethyl ether to yield purified product with 78% yield.

2.2.5. Synthesis of graphene oxide

Graphene oxide was synthesized from graphite powder using improved hummers method [22]. In brief, 1 g graphite was mixed with 200 mL acid mixture containing H₂SO₄ and H₃PO₄ with a 9:1 vol/vol ratio, respectively, under constant stirring. After steady addition of 6 g KMnO₄, the mixture was let to stir for 3 days in 50 °C. The solution was poured into ice water and then H₂O₂ solution was added dropwise till the color of the suspension changed to bright yellow. The obtained graphite oxide solution was centrifuged and washed twice with 1 M of HCl aqueous solution and then three times with deionized water to set the pH value of the solution to 4–5. Graphene oxide sheets were separated by centrifugation and freeze-dried (Tajhizat Sazan Pishtaz Co, Iran).

2.2.6. Synthesis of alkynyl-GO

In order to utilize the click reaction in the next steps of this work, we had to modify the surface of the GO with alkynyl groups. Alkynyl-GO was prepared using propargyl amine. In a typical procedure [23], GO (0.1 g) was dispersed in 5 mL DMF using Bandelin probe sonicator (20 min, 50%, 5 s on/3 s off). Propargyl amine (0.268 g, 2.73 mmol) was added into the GO suspension and dissolved using stirrer. DCC (4 g, 20.87 mmol) and DMAP (0.3 g, 2.46 mmol) were gradually poured into the mixture during 20 min. The reaction solution was let to stir for 16 h at room temperature. After the completion of reaction, the suspension was diluted in 30 mL of DMF. The diluted suspension was centrifuged and washed thoroughly using DMF and then dried under vacuum overnight to produce 0.207 g alkynyl-decorated GO.

2.2.7. Synthesis of Janus poly(ε -caprolactone)-graphene oxide-poly(NIPAAm-co-AAm-co-AA) (J-(PCL-NGO-terpolymer))

J-(PCL-NGO-Terpolymer) was prepared using Pickering oil in water (O/W) emulsion/solvent evaporation method. Briefly, azideterminated PCL (20 mg) was dissolved in DCM (2 mL) to form the oil phase. On the other hand, alkynated-GO (10 mg) was dispersed in 10 mL phosphate buffer saline (PBS) (pH adjusted to 7.4) and sonicated for 30 min (5 s on/3 s off) to obtain a homogeneous colloidal suspension of GO nanosheets (NGO) as water phase. Afterwards, a 2 mL orange colored aqueous solution containing ascorbic acid (21.13 mg, 0.12 mmol), sodium bicarbonate (30.2 mg, 0.12 mmol) and 10 mg of copper(II) sulfate pentahydrate was added to the aqueous phase. Oil phase was then added dropwise to an emulsifier-free aqueous solution containing NGO. Oil-in-water (O/ W) micro-emulsion was formed and was let to stir for 16 h at room temperature to produce one side PCL coated graphene oxide J-(PCL-NGO). Terpolymer (50 mg) was added to the reaction solution and stirred for a day at room temperature. After the completion of reaction, the mixture was kept at room temperature for 24h to evaporate the organic solvent and form *J*-(PCL-NGO-Terpolymer). The product was washed once with DCM and twice with distilled water. The resultant material was freeze-dried to remove the trapped water without destroying the nanoparticle structures.

2.2.8. Synthesis of mixed poly(ε -caprolactone)-graphene oxide-poly(NIPAAm-co-AAm-co-AA) (m-(PCl-NGO-terpolymer))

GO (10 mg) was dispersed in 10 mL DMF, using Bandelin probe sonicator (20 min, 50%). CuBr (15 mg) and PMDETA (22 μ L) were successively added into the GO suspension and dissolved by stirring. Azide containing PCL and terpolymer were added simultaneously to the mixture and the reaction solution was let to stir for 48 h at room temperature. After the reaction was completed, the obtained m-(PCL-NGO-Terpolymer) was centrifuged and washed thoroughly using DMF and water, then dried overnight under vacuum.

m-(PCL-NGO) and J-(PCL-NGO) samples were synthesized in the

absence of terpolymer through this method separately for TEM analysis.

2.3. Characterization and equipment

Polymers were characterized using Fourier transform-infrared spectroscopy (Bruker-Equinox55 FT-IR) and ¹H NMR (Bruker, 500 MHz). ¹H NMR spectrum of azide-terminated PCL and terpolymer were recorded in CDCl₃ and D₂O, respectively. The number averaged molecular weight (Mn) of azide-terminated PCL was calculated with ¹H NMR data. Number average molecular weight (Mn), weight average molecular weight (Mw) and polydispersity index (PDI) of poly (NIPAAm-co-AAm-co-AA) were determined in tetrahydrofuran containing 0.25% of TBAB at 25 °C and in the flow rate of 0.7 mL/min by gel permeation chromatography (GPC) using a PL-EMD 950 instrument. Calibration was carried out with monodisperse polystyrene standards. GPC was used to determine Mn, Mw and PDI of PCL, too. PCL was dissolved in tetrahydrofuran and GPC was run in the flow rate of 1 mL/min at 25 °C. The morphology of GO and functionalized GO were investigated by transmission electron microscopy (TEM) (Zeiss LEO 906 TEM instrument) and scanning electron microscopy (SEM) (FESEM; Zeiss SuprATM 55, Germany). The materials were dispersed in distilled water and one drop of the dispersed mixture was placed on a carbon coated grid. The grid was completely dried and used for TEM/SEM analysis (150 kV). Thermal gravimetric analysis (TGA) was performed to display the content of polymer on graphene oxide surface (TGA Q50 V6.3 Build 189). Samples were heated at a rate of 20 °C/min under nitrogen blanket and the data was recorded from 20 to 600 °C. The X-ray diffraction (XRD) patterns were obtained on an X-ray diffractometer (X'Pert PRO MPD, PANalytical Company, Netherlands) with Cu Ka radiation. The topography of the GO nanosheets was characterized by atomic force microscopy (AFM, Auto Probe CP Research- Veeco Instruments Inc., USA) on a freshly cleaved mica substrate. The drug release was studied using ultraviolet-visible light (UV-Vis) spectrophotometer spectra (Perkin-Elmer Lambda 25 spectrophotometer). Cloud point temperature (Tcp) was determined using an UV-Vis spectrophotometer coupled with a temperature controller. The polymer solutions were prepared using standard phosphate buffer (PBS, pH = 7.4). The heating rate was 2 °C/10 min and 0.2 °C/10 min near the cloud point (CP). From the calibration curve based on normalized absorbance vs. temperature, CP was determined as the temperature in which the absorbance is 10%. The volume phase transition temperature, VPTT, of the "Janus" and "mixed" nanoparticles were investigated using a micro-differential scanning calorimeter (VP-DSC, Micro Cal Inc.). The micro-DSC were measured from 20 $^{\circ}$ C to 80 °C at a heating rate of 1 °C/min under a nitrogen atmosphere with 0.1% (W/V) of each nanoparticle in aqueous solution. The average hydrodynamic diameter, size distribution and surface charge) (zeta potential) of aqueous dispersion of all nanoparticles were determined by dynamic light scattering (DLS) (Nano ZS, malven instrument, UK) at 25 °C. Morphological assessment of nanoparticles after loading fluorescein as a hydrophobic dye was performed with a Zeiss light microscope. 10 mg of mixed and Janus nanoparticles were dispersed in 10 mL acetone and then 1 mg of fluorescein, as a fluorescent tracer, was added to the above suspension. After 1 h, a few drops of suspension were diluted, transferred to a lamella and allowed to dry.

2.4. Drug loading and encapsulation efficiency

10 mg of each nanocarrier (*m*-(PCL-NGO-Terpolymer) and *J*-(PCL-NGO-Terpolymer)) was separately dispersed in a mixture of deionized water (5 mL) and DMF (5 mL). 1 mg 5-FU as hydrophilic

anti-cancer drug and 1 mg quercetin as hydrophobic one were added into the dispersions. The mixture was incubated for 48 h to prepare drug loaded nanocarriers. Drug loaded nanocarriers were separated from the solution by centrifuging the mixture and were washed twice with solvent to remove unloaded drug molecules. The product was freeze-dried for 36 h in order to obtain dried drug loaded nanocarriers without any agglomeration. Single drug loading, *i.e.* 5-FU or quercetin, was carried out according to the procedure described above and was used to yield 5-FU or quercetin loaded *J*-(PCL-NGO-Terpolymer) nanoparticles. Dried solid nanoparticle samples were obtained after lyophilization.

Drug loading and encapsulation efficiencies of these nanoparticles were determined by UV–Vis spectrophotometer. A predetermined amount of dried nanocarriers were dissolved in DMF/ $\rm H_2O$ (1:1) to determine the amount of encapsulated drug. The DMF/ $\rm H_2O$ mixture could instantaneously dissolve both polymers and consequently, the entrapped quercetin and 5-FU immigrate into solvents media suddenly, and the residue of nanoparticles were separated by high speed centrifuge. The absorbance of the supernatant was determined by UV–Vis spectrophotometer (287 nm for 5-FU and 376 nm for quercetin) in accordance with the standard calibration curve of drug in solvent (1:1 DMF/ $\rm H_2O$). Encapsulation efficiency (EE) and drug loading (DL) were calculated according to the following equations (Eqs (1) and (2)):

$$DL(\%) = \frac{\textit{Weight of drug entrapped within nanoparticles}}{\textit{Total weight of nanoparticles}} \times 100$$
 (1)

$$\textit{EE\%} = \frac{\textit{Weight of drug entrapped within nanoparticles}}{\textit{Total drug added}} \times 100$$
 (2)

2.5. In-vitro release of drugs from nanocarrier

In-vitro release profiles of 5-FU and quercetin from mixed and Janus nanoparticles were performed in phosphate buffer solutions of 7.4 at 37 and 40 °C. The same amount for every sample (1.5 mg) was dispersed in 2 mL PBS and transferred to a dialysis bag (molecular weight cut off 12 KD). The bag was then immersed into the flask containing 60 mL PBS (pH = 7.4), and was stirred at 100 rpm at 37 and 40 °C. At determined time intervals, 2 mL of the sample was taken out from the release media and replaced with fresh buffer (2 mL). The amount of released quercetin and 5-FU in PBS media were determined by UV—Vis spectroscopy, at wavelengths of 202 nm and 260 nm, respectively. The drug release percentage can be determined according to Equation (3):

Drug release (%) =
$$M_t/M_0 \times 100$$
 (3)

2.6. Cell cytotoxicity assay

The relative cell viability was evaluated in the presence of quercetin, 5-FU, quercetin/5-FU, *J*-(PCL-NGO-Terpolymer), quercetin-loaded *J*-(PCL-NGO-Terpolymer), 5-FU-loaded *J*-(PCL-NGO-Terpolymer), (quercetin/5-FU)-loaded *J*-(PCL-NGO-Terpolymer) and mixed (quercetin/5-FU)-loaded *m*-(PCL-NGO-Terpolymer) rat C6 glioblastoma and OLN-93 cells (rat brain non-tumor cell line) *via* conventional 3-(4,5-dimethylthiazol-2-yl)-2,5-diphenyltetrazolium bromide (MTT)

assays. The cells were seeded at the density of 5×10^3 cells per well in 96-well plates and incubated at $37\,^\circ C$ in a humidified atmosphere containing 5% CO $_2$ for 24 h. After pre-incubation, cell culture was removed and cells were treated with $100\,\mu L$ fresh medium, containing either above-mentioned samples at various concentrations for 24 h and at two temperatures, 37 and $40\,^\circ C$. The control and treated cells were observed and photographed using an inverted phase contrast microscope (BEL, Italy) equipped a camera. 1 mM freshly-prepared MTT was added to each well and the samples were incubated for 4 h at desired temperatures. Then, the culture media were removed and $100\,\mu L$ DMSO was added to each well. Prepared samples were incubated for 10 min at $37\,^\circ C$. The absorption of obtained solution was measured at 540 nm.

3. Results and discussion

Poly(ε-caprolactone) and (*N*-isopropylacrylamide-*co*-acrylamide-co-allylamine) terpolymer were synthesized by ring opening polymerization (ROP) and free radical polymerization. GO was synthesized by improved Hummers method and was functionalized with alkynyl groups. Then, alkynyl-GO was modified with PCL and terpolymer via two methods. First method was oil-in-water microemulsion method in which dichloromethane and PBS were used as organic and aqueous layers, respectively. In this technique, alkynyl-GO works as an emulsifier. PCL in the oil phase was reacted with the internal sides of alkynyl-GO and the external sides of alkynyl-GO were functionalized with terpolymer. In this reaction, "lanus" nanoparticles were produced as a specific kind of nanoparticles. In the second method for functionalization of alkynyl-GO. DMF was used as a sole organic solvent to disperse alkynyl-GO and dissolve both polymers. Under this condition, two different types of polymers will be grafted on both surfaces of graphene oxide disorderly named "mixed" nanoparticles (Fig. 1).

3.1. Preparation and characterization of hydrophobic and hydrophilic domains of nanoparticles

The initiator, containing azide group, was initially prepared for $poly(\epsilon$ -caprolactone) synthesis. 1-Chloro-2-hydroxy-3-azido propane (azidated epichlorohydrin) was synthesized using epichlorohydrin and sodium azide in the presence of tetrabutylammonium bromide as a phase-transfer catalyst (Fig. 2, **Step 1**).

Fig. 3a shows FT-IR spectrum of azidated epichlorohydrin. The intense absorption at $2088\,\mathrm{cm^{-1}}$ and a characteristic peak at $1267\,\mathrm{cm^{-1}}$ are attributed to azide and CH₂-Cl groups, respectively. The wide absorption at $3413\,\mathrm{cm^{-1}}$ is attributed to OH stretching bond.

N₃-PCL was synthesized via ring opening polymerization of ε-caprolactone in the presence of azidated epichlorohydrin as initiator and Sn(Oct)₂ as catalyst at 120 °C (Fig. 2, Step2). FT-IR spectrum of azide-terminated PCL is illustrated in Fig. 3b. The PCL characteristic peaks were located at 1721 and 1172 cm⁻¹, related to C=O and C-O stretching bonds of esteric groups, respectively. The absorption band at 2943 cm⁻¹ corresponds to C-H stretching bond and that at 2103 cm⁻¹ belongs to the azide end groups. Presence of these peaks confirms the formation of azide-terminated PCL chain. As well as, four major peaks related to the repeating units of PCL (d, e, f and g), three small but discernible peaks (a, b and c) are observable in the ¹H NMR spectrum of azide-terminated PCL in CDCl₃ (Fig. 3c) which is related to azidated epichlorohydrin (AE). The methylenic proton resonance peaks of PCL chains appear as multiple peaks at 1.3 (f), 1.6 (e), 2.3 (d) and 4 (g) ppm. The peaks related to the protons of the used initiator can be detected at 4.1 (c), 3.7 (b) and 3.2 (a) ppm. The number average molecular weight of azide-terminated PCL was calculated from peak area ratio at

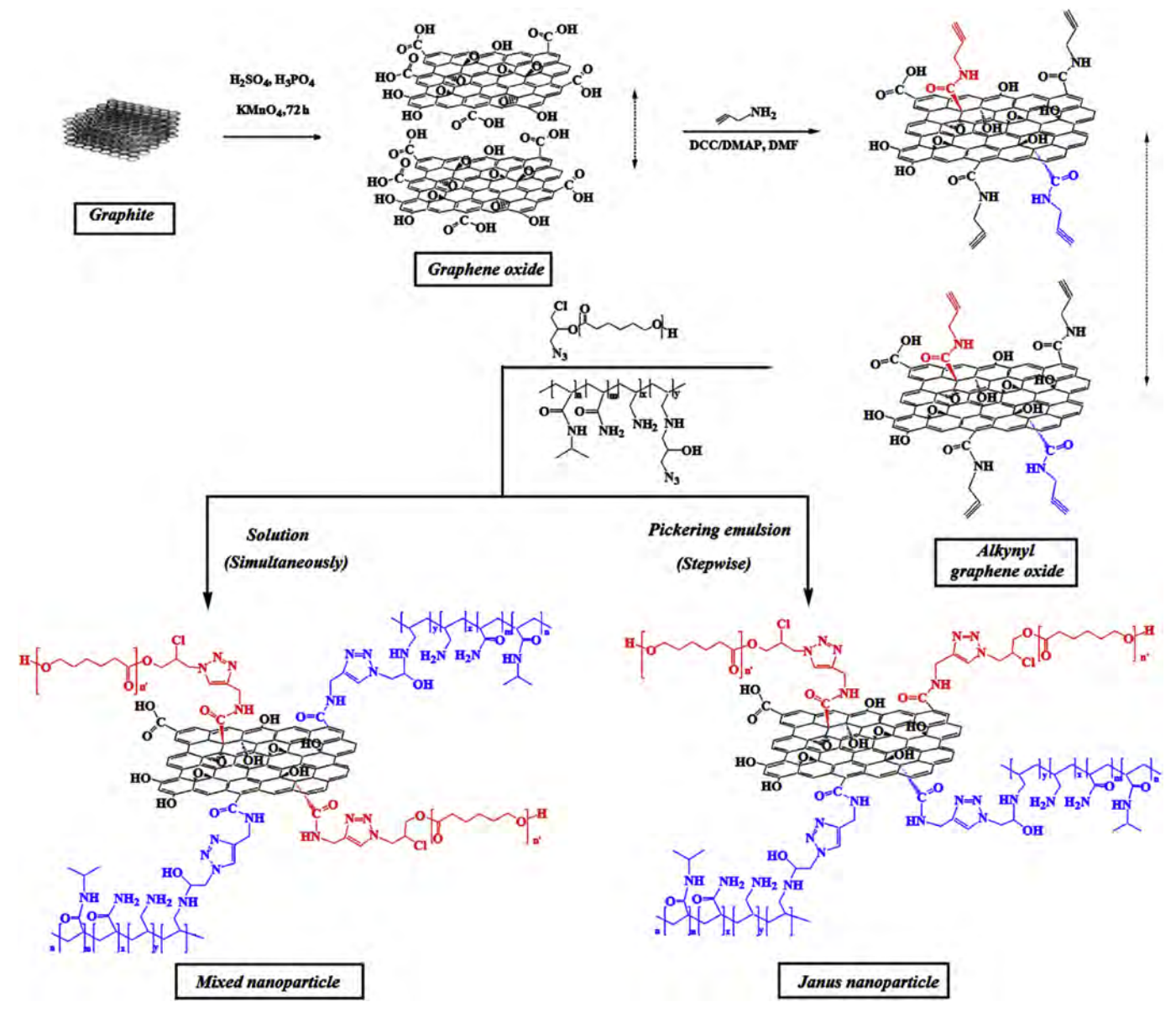


Fig. 1. Synthesis of GO, Alkynyl-GO, Mixed and Janus nanoparticles.

1.3 ppm (peak "f" of PCL) and 3.7 ppm (peak "b" of AE). According to the integral values of these two peaks, number average molecular weight of PCL is about 2350 g/mol. GPC results of PCL showed that Mn and PDI were 2030 g/mol and 1.13, respectively.

Poly(*N*-isopropylacrylamide) and its copolymers are the most relevant thermo-responsive polymers, because it possesses a cloud point temperature (Tcp) that makes it an appropriate nanovector for smart delivery of the drug only at the target site. Tcp of pure PNIPAAm is around 32 °C in aqueous solutions and to have a polymer with a Tcp value closely similar to the cancer cell temperature, some extra monomers should be applied to increase this temperature. Here and similar to the previously reported procedure [24], acrylamide and allylamine were used as co-monomers for adjusting the Tcp value of PNIPAAm, and thus, the theoretical molar ratio of NIPAAm:AAm:AA was selected to be 15:0.75:1 (sample T₂). Consequently, poly(NIPAAm-co-AAm-co-AA) was synthesized through free radical polymerization using AIBN as initiator according to Fig. 2, **Step3**. FT-IR spectrum of terpolymer is shown in

Fig. 4a. C=O stretching vibration of amide group can be seen as a peak at 1635 cm⁻¹ and the peaks at 1453 and 3293 cm⁻¹ are ascribed to N-H bending and stretching vibration frequency, respectively. C-H stretching bond in terpolymer appeared as a tiny sharp peak at 2969 cm⁻¹. Peaks at 1455 and 1387 cm⁻¹ indicate the methylene groups of the main polymer chain and isopropyl group of NIPAAm, respectively.

¹H NMR spectrum of terpolymer is shown in Fig. 4c. Characteristic peaks of the backbone protons are 1.43 (c) and 1.87 (d) ppm. The broad peaks at 7.68 (g) and 7.93 (h) ppm, respectively indicate primary and secondary amide groups in acrylamide and *N*-isopropylacrylamide. Furthermore, the proton resonance peaks related to the amine groups in allylamine appeared at 3.42 (e) and 3.50 (f) ppm. These peaks affirm the existence of all three monomers in the terpolymer structure. The molecular weight and polydispersity index of the terpolymer were measured by gel permeation chromatography (GPC). The results showed that the number average and the weight average molecular weights were

Fig. 2. Synthesis of azidated epichlorohydrin (Step 1), azide-terminated PCL (Step 2), Terpolymer (Step 3) and Azidated Terpolymer (Step 4).

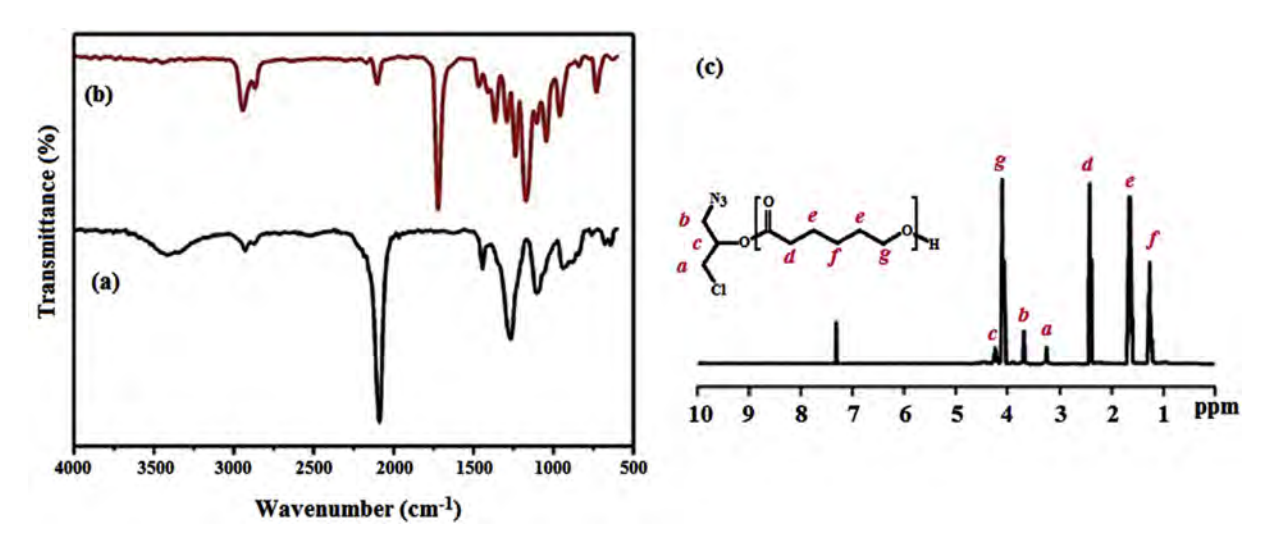


Fig. 3. FT-IR spectra of azidated epichlorohydrin (a), azide-terminated PCL (b) and ¹H NMR spectrum of azide-terminated PCL (c).

9983 and 14176 g/mol, respectively. The PDI of terpolymer was 1.42 which is a relatively modest value.

Terpolymer was azidated in the presence of AE and triethylamine at $50\,^{\circ}\text{C}$ (Fig. 2, **Step 4**). Coupling of azidated epichlorohydrin and terpolymer has been confirmed using FT-IR (Fig. 4b). Stretching vibration of azide groups attached to terpolymer can be seen at $2102\,\text{cm}^{-1}$.

To evaluate the relationship between the Tcp values of the azidated terpolymer solutions at two different media (water and buffer) and the monomer ratios of the corresponding terpolymers, UV—Vis spectrophotometer coupled with a temperature controller was used. As shown in Fig. 5, variation in the investigated media

exhibits a significant change in the Tcp transition, which sensitively depends on the type and concentration of salts used in buffer. In PBS media a sharp phase separation was observed at 35.90 °C (Fig. 5), which is lower than the desired value. As monomer content in terpolymer has direct relationship to Tcp and in order to increase the Tcp value, two more formulations were prepared similar to the above polymerization method, except that the weight percentages of three monomers were changed according to Table 1. Strikingly, the exact same trend is also observed in the Tcp values of azidated terpolymer in water and PBS media and suggests that the solvent must play a determining role in Tcp transitions.

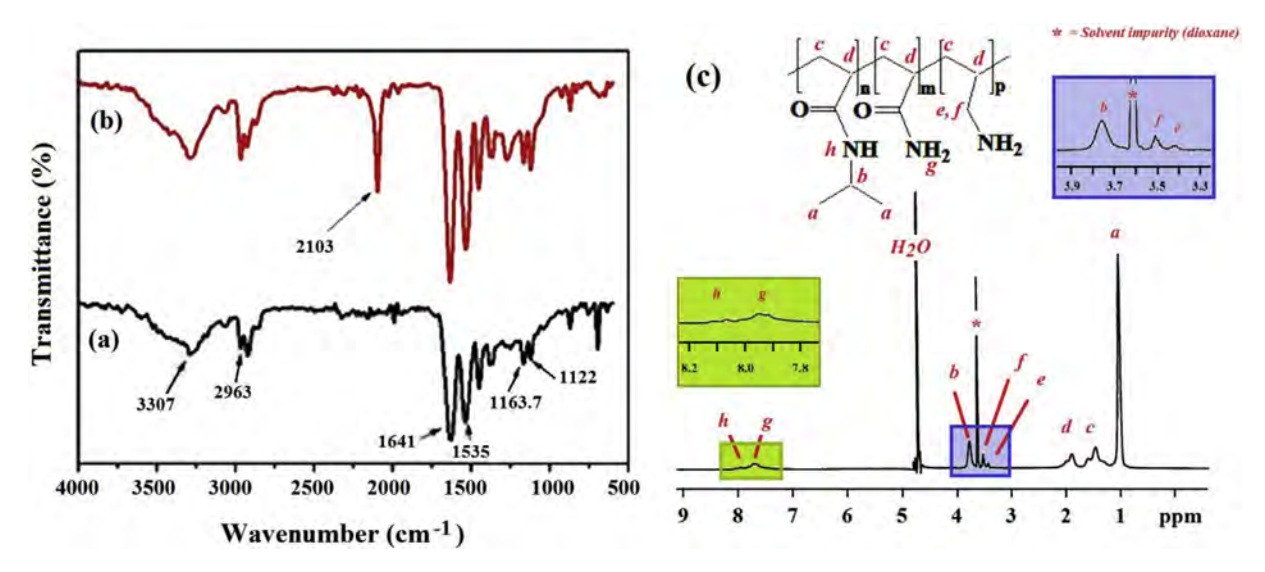


Fig. 4. FT-IR spectrum of terpolymer (a), azidated terpolymer (b) and ¹H NMR spectra of terpolymer in D₂O (c).

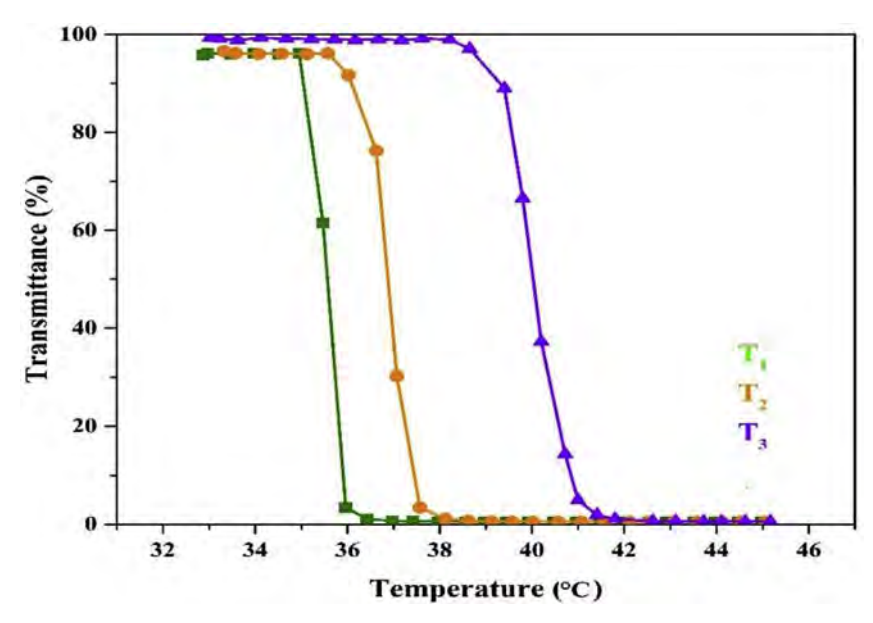


Fig. 5. Tcp profile of azidated terpolymer in PBS at different ratio of monomers (Table 1).

Table 1 Influence of feed monomer ratio on the Tcp.

Sample	% mole ratio in the feed			Tcp (°C) ^a	
	NIPAAm	Aam	AA	pH = 7.4	H ₂ O
T ₁	17	1	1	35.90	39.10
T_2	15	0.75	1	37.50	43.00
T_3	10	1	1	41.02	46.30

 $^{^{\}rm a}\,$ The concentration of terpolymer solution always being 1%, w/v.

3.2. Preparation and characterization of alkynylated GO

The focus of this paper is to synthesize Janus nanoparticles through the reaction of each surface of nano-graphene oxide (NGO) with two different polymers. So, [2+3] click reaction has been selected to provide this purpose and accordingly, the alkynated graphene oxide, azide-terminated poly(ε -caprolactone) and

azidated poly(NIPAAm-co-AAm-co-AA) were designed. Indeed, it was found that GO can locate between aqueous and oil phases and can act as an emulsifier to create stable submillimeter-sized oil droplets in water [25]. However, freshly prepared GO revealed little surface-active properties in water, and GO sheets started to appear as a colloidal surfactant just after a few hours, which is due to their large size and high molecular mass. To overcome this drawback in this work, we designed a mass reducing process using probe sonicator to accelerate the migration of GO sheets to the surface as well as convert millimetric droplets to nanometric ones.

As shown in Fig. 1, graphene oxide was synthesized by oxidation of graphite via improved hummer's method, introduced by Marcano et al. [22]. They showed that increasing the amount of KMnO₄ and using a mixture of H_2SO_4/H_3PO_4 can improve the oxidation process.

FT-IR analysis was done to characterize the nature of the GO surface (Fig. 6a). The broad band at approximately $3300-3500\,\mathrm{cm}^{-1}$ is attributed to the stretching vibration of OH

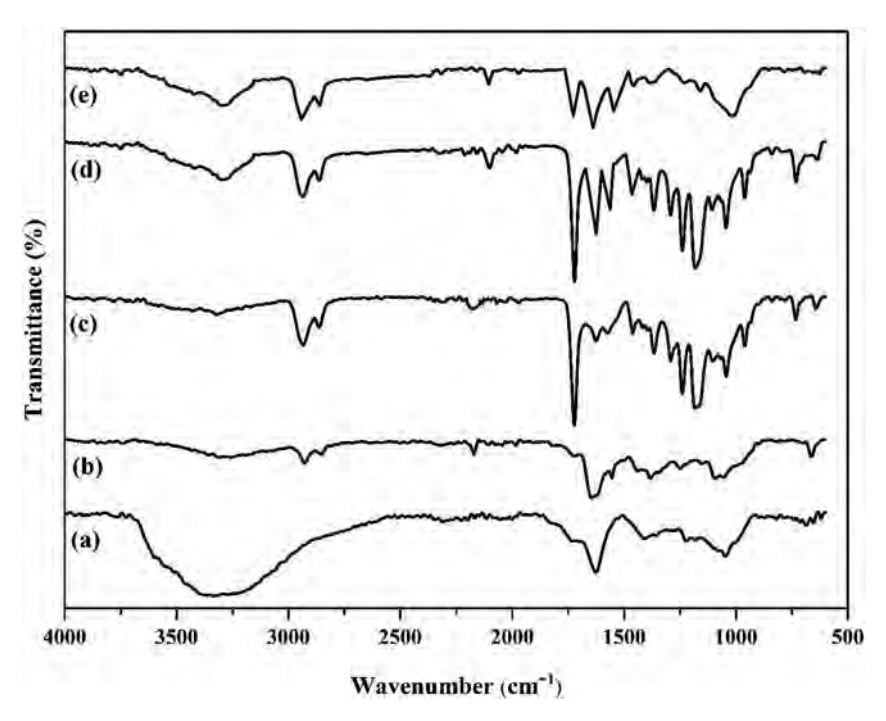


Fig. 6. FT-IR of GO (a), alkynyl-GO (b), J-(PCL-NGO) (c), J-(PCL-NGO-Terpolymer) (d) and m-(PCL-NGO-Terpolymer) (e).

group. The appearance of the absorption bands at 1725, 1626 and $1223~{\rm cm}^{-1}$ is assigned to C=O, C=C and C-O stretching vibrations of the carboxylic, aromatic hydrocarbon, and epoxy groups, respectively.

Alkynylated GO was then prepared after amidation of the GO carboxylic acids with propargyl amine (Fig. 1). Several new peaks appeared in the FT-IR spectrum of alkynyl-GO. The characteristic peaks of amide (-C(O)NH-) stretching vibration appeared at $1560\,\mathrm{cm}^{-1}$ and indicates the presence of the amide bond which was formed through the reaction between GO and propargyl amine. Moreover, methylene ($-CH_2-$) stretching vibration can be observed at 2926 and 2853 cm $^{-1}$ (Fig. 6b).

3.3. Preparation of Janus (PCL-NGO-terpolymer) and mixed (PCL-NGO-terpolymer) nanoparticles

As illustrated in Fig. 7 (step 1), J-(PCL-NGO-Terpolymer) nanoparticles were prepared via solvent evaporation of spontaneously formed oil-in-water microemulsion. In this system, oil phase contained azide-terminated PCL, water phase contained azidated terpolymer and graphene oxide was used as the emulsifier. Oil phase was dispersed in water through stirring to make oil droplets. Graphene oxide acts as a surfactant and forms a monolayer at the interface between oil and water to stabilize the emulsion. Alkyne groups in both sides of the graphene oxide would face either oil or water phase [26]. NGO alkyne groups that face to oil phase were activated using sodium ascorbate (sodium bicarbonate + ascorbic acid) and copper (II) sulfate pentahydrate to react with oil-solvated azide-terminated PCL. Alkyne groups facing water phase would react with water-solvated azidated terpolymer via click reaction in the presence of copper and ligand to form triazole ring and graft azidated poly(NIPAAm-co-AAm-co-AA) on the graphene oxide surface.

To confirm the conjugation of azid-terminated PCL on the surface of graphene oxide, the reaction was stopped at the first step before adding azidated terpolymer and the sample was evaluated using FT-IR (Fig. 6c). Compared with alkynyl-graphene spectrum,

the strong vibration at 1721 cm⁻¹, relating to ester carbonyl stretching (C=O) as well as the appearance of PCL pattern in the FT-IR spectrum of one-side polymer attached GO would confirm the grafting of PCL on the surface of graphene oxide.

Janus nanoparticles (*J*-(PCL-NGO-Terpolymer)) have been characterized using FT-IR (Fig. 6d). Compared with *J*-(PCL-NGO) spectrum (Fig. 6c), the peaks at 3251, 1624 and 1550 cm⁻¹, respectively relating to N-H stretching vibration frequency, C=O stretching vibration of amide group and N-H bending vibration frequency, have become stronger. The weak peak at 2101 cm⁻¹ ascribes to the unreacted azide groups on terpolymer chains. Presence of peaks relating to these groups confirms the conjugation of azidated terpolymer on the surface of graphene oxide. The peak at 2173 cm⁻¹ for alkyne group of propargyl amine has been disappeared, showing that the conjugation has been performed *via* click reaction.

A mixture of azide-terminated PCL and azidated terpolymer can be randomly grafted on the surfaces of graphene oxide in a common solvent to make mixed nanoparticles. To perform the click reaction, copper bromide and PMDETA were used in DMF. Both polymers were linked on the surface of GO through their azide heads in a one-step reaction to produce mixed nanoparticles (Fig. 7, Step 2).

Compared with FT-IR spectrum of Janus nanoparticle (Fig. 6d), the spectrum of mixed nanoparticle (Fig. 6e) shows all important absorptions of various functional groups present in the structure of nanoparticle, but with different intensities. In Janus morphology, there is a distinct band at 1721 and 1624 cm⁻¹ (corresponding to the PCL and terpolymer carbonyl groups), while for the mixed one there is a broad band in this region. Due to the interactions between the functional groups of PCL and terpolymer units in the mixed structure, these bands become wide, while these interactions are not so important in the separated structure of Janus form. This difference between two morphologies is similar to the pattern observed in block and random copolymers [27].

Thermogravimetric analysis is a good complementary technique which can determine the changes in thermal stability of the Janus

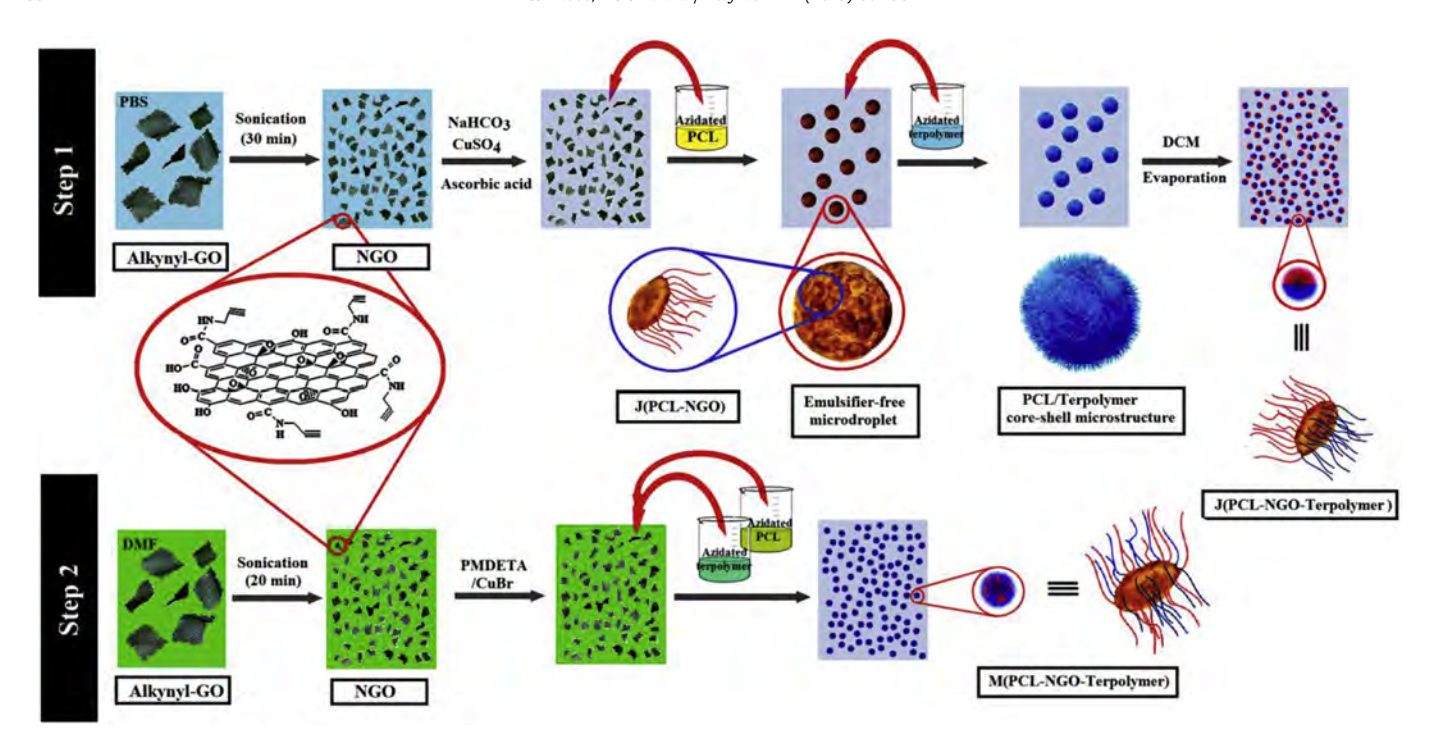


Fig. 7. Illustrated method for formation of "Janus" nanoparticle (Step 1) and "mixed" nanoparticle (Step 2).

and mixed structure of (PCL-NGO-Terpolymer). TGA curves of graphene oxide (black), J-(PCL-NGO-Terpolymer) (red) and m-(PCL-NGO-Terpolymer) (blue) are shown in Fig. 8A. In the pure GO sample CO, CO₂ and vapor from the most labile functional groups are released during a single weight loss event between 200 and 220 °C relating to pyrolysis of unstable oxygen-containing functional groups (Fig. 8a). However, a small mass loss below 100 °C relates to water evaporation. The major weight loss was started at 120 °C and at temperatures below 600 °C a total weight loss of about 67% was observed. In contrast, both modified NGO with either Janus or mixed structures showed higher thermal stability than pure graphene oxide. Actually, the weight loss curve of modified NGO shows the amount of grafted polymer onto the surface of NGO after each step of functionalization.

Functionalizing NGO with azide-terminated PCL and azidated

terpolymer would impressively enhance thermal stability of NGO sheets, which is due to the role of PCL and terpolymer as a barrier against heat. m-(PCL-NGO-Terpolymer) lost 51% of its weight from 230 °C to 600 °C which is related to the decomposition of conjugated polymers, while J-(PCL-NGO-Terpolymer) lost only 43% of its weight in this region (Fig. 8b and c). Around 360 °C, the plots for both Janus and mixed samples have notable drops, which indicates degradation of the conjugated polymers from the surface of both nanoparticles. This slump is more significant for the Janus particles, which is due to the difference in particle structure.

Usually homopolymer of polyallylamine shows three distinct regions of weight loss. The first one, which is below $150\,^{\circ}$ C, is related to the release of bound water in the polymer matrix. The second between 150 and 370 °C corresponds to the scission of the amine side-chains. The last weight loss around $370-550\,^{\circ}$ C is

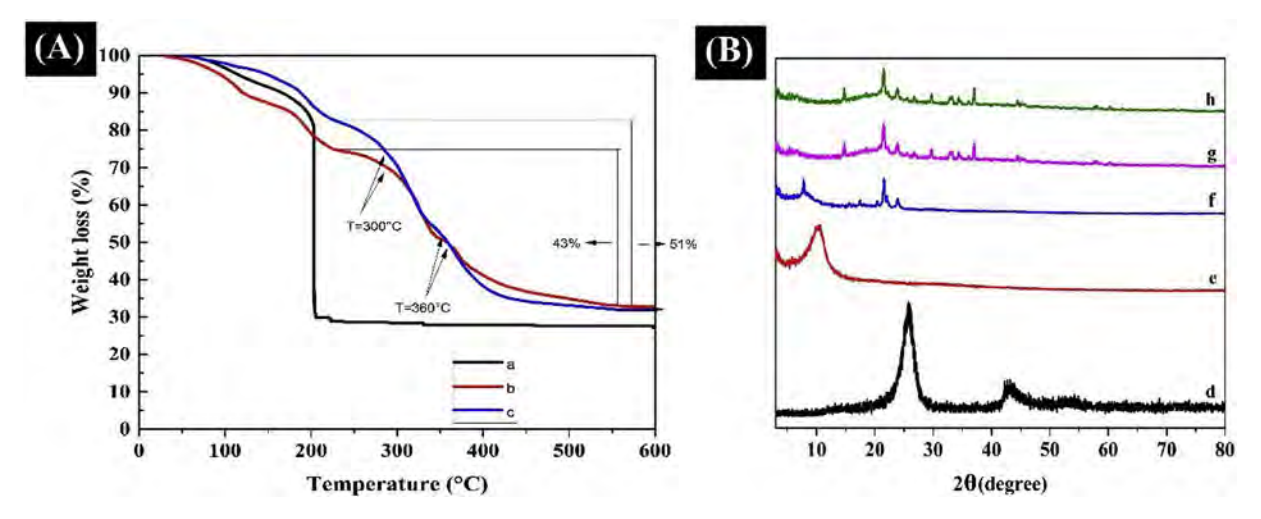


Fig. 8. (A): TGA thermograms of GO (a), J-(PCL-NGO-Terpolymer) (b) and m-(PCL-NGO-Terpolymer) (c); (B): XRD diffractograms of graphite (d), GO (e), J-(PCL-NGO-Terpolymer) (g), m-(PCL-NGO-Terpolymer) (h).

attributed to the polymer chain scission [28]. Similar to polyallylamine, polyacrylamide also showed an explicit weight loss as soon as heating was started. During this process, the adsorbed water was isolated and this event was completed below 100 °C. Separation of carbon dioxide from pendant groups of polyacrylamide was also detected below 200 °C and as the temperature raised more, the degradation of the polymers began [24]. TGA measurements provide valuable information that can be used to prove the formation of Janus nanoparticle. The overall TGA curves indicate that thermal stability of the mixed nanoparticles is higher than Janus ones. The proximity of polyacrylamide chains in Janus nanoparticles promotes higher polymer-polymer interactions, which naturally results in lower chain mobility. By heating the nanoparticle, the retained energy will be released and accordingly, lower temperature is needed for degradation of Janus nanoparticle. TGA of mixed nanoparticles demonstrates that an additional amount of energy is needed for further degradation which is due to the inaccessibility of reactive sites of polymer chains to each other and consequent lower amount of hydrogen bonding.

Micro DSC heating curves of Janus and mixed nanoparticles in aqueous solution shows the switch-ability of the polymeric shell and the temperature sensitivity of the whole nanoparticles. As we described above, volume phase transition temperature (VPTT) of azidated terpolymer in buffer solution was about 37.5 °C (T_2 sample). This VPTT will be changed by incorporation of hydrophobic PCL and hydrophilic NGO in nanoparticle structure. Mixed nanoparticle shows a similar temperature-sensitive behavior in buffer media as Janus nanoparticles (i.e. $40\,^{\circ}$ C), but with slightly higher critical temperature of about $42\,^{\circ}$ C, higher than Tcp of azidated terpolymer. The higher VPTT of nanoparticles in contrast to Tcp of azidated terpolymer arises from the hydrophilic nature of graphene oxide.

Crystallographic structure of the nanoparticles series was determined by X-ray diffraction (Fig. 8B). In X-ray diffraction pattern (XRD), graphite shows a characteristic peak at $2\theta = 26^{\circ}$ (Fig. 8d). XRD of graphene oxide showed a distinct peak at $2\theta = 10.28^{\circ}$, which is related to the interlayer spacing of GO layers that is about 8.60 Å (Fig. 8e). XRD pattern of the as-prepared J-(PCL-NGO) showed a sharp peak at 2θ of 7.76°, indicating the interlayer distance of 11.38 Å. The shift of XRD peak of NGO from 10.28° to 7.76° in one-side coated NGO suggested that the polymeric NGO has been separated well. However, some new peaks at 21.52° and 23.87° relating to PCL chains were observed in the XRD pattern of J-(PCL-NGO) structure (Fig. 8f). In the XRD patterns of Janus and mixed nanoparticles, multi-peaks of terpolymer in several 2θ shifts appeared in addition to the PCL chains peaks. Weak peak of GO at 5.82° revealed that the interlayer spacing was approximately 15.17 Å (Fig. 8g and h). 2θ shift and spacing increase for GO interlayer demonstrate the placement of polymer chains between GO layers and exhibit higher extent of modification in comparison with alkynated NGO.

The functionalized NGO morphology was investigated using scanning electron microscopy (SEM) and transmission electron microscopy (TEM). SEM ascertained different morphologies of nanoparticles obtained from different synthetic methods. SEM image of graphite shows a dense morphology (Fig. 9a), while, the presence of extensive peel-like feature in the graphene oxide sample proves the oxidation of graphite (Fig. 9b). The image of asprepared Janus nanoparticles (without washing and drying after the reaction) exhibits clearly semi-individual particles with bright and dark contrast (Fig. 9c), whereas a sheet morphology was observed for the mixed nanoparticle. After drying the nanoparticles, the mixed one displayed a continuous layered morphology (Fig. 9g and h), while, several partitioned fluffy domains could be identified in the Janus nanoparticles (Fig. 9d and e).

We believe this behavior in Janus nanoparticle is based on two important features: (i) the hydrophobic interaction between the PCL chains, which results in the self-assembly of nanoparticles to form micrometer-sized core, and (ii) the hydrophilic chains on the periphery of the macrocluster, which are designed from the interaction between azidated terpolymer faces of several Janus nanoparticles to optimize the repulsive interactions. In this case, the implementation of two different hydroaffinities in two dissimilar sides of the nanoparticle favors the arrangement with directional growth, resulting in the formation of hierarchically organized supramolecular microarchitectures. Such an aggregation pattern cannot be seen in the case of mixed nanoparticles. In the mixed nanoparticles, the conjugated polymers have been settled side-byside and form a unified structure without any aggregation or clustering.

To further examine the structure of superstructure particles *via* the self-assembly of the Janus nanoparticles, TEM analysis was conducted to determine the morphology and arrangement of the materials (Fig. 10). Through TEM images, GO and NGO sheets can be distinguished as smooth rippled surfaces with wrinkled edges (Fig. 10a and b, respectively). It is observable that GO sheets have completely been surrounded by a continuous wrinkled layer (Fig. 10a) and these micrometric scaled materials have been converted to the nanometric structures with discontinuous wrinkled by ultrasonication shearing (Fig. 10b). Interestingly, Fig. 10c and d clearly show smart growth of the polymeric layer on one side of graphene oxide and as indicated by the arrow in the TEM micrographs, bare surfaces could be found on the other side. PCL can be seen as granular, and terpolymer particles can be observed as a condensed dark layer. TEM images of m-(PCL-NGO) and m-(NGO-Terpolymer) in its solid form exhibited high surface coverage and consequently, high level of grafting as compared to their own Janus forms. PCL granules and cloud-like terpolymer are present all around both sides of NGO sheet (Fig. 10e and f). Comparing TEM images in Fig. 10g with 10 h reveals that various synthesis methods of J-(PCL-NGO-Terpolymer) and m-(PCL-NGO-Terpolymer) would lead to different morphologies. TEM image in Fig. 10e clearly demonstrates that azide-terminated PCL has grafted to NGO from one side and azidated terpolymer has conjugated from the other side. In Fig. 10f, azide-terminated PCL and azidated terpolymer have irregularly been spread on both sides of NGO sheet. This affirms that Janus nano-graphene oxide can be prepared via Pickering emulsion polymerization to have one side covered with PCL while, the other side reacts with terpolymer. In this process, NGO nanosheets act as the surfactant and the emulsion polymerization is emulsifier-free.

Atomic-force microscopy (AFM) was performed for NGO, J-(PCL-NGO-Terpolymer) and *m*-(PCL-NGO-Terpolymer). Thickness of bare NGO is about 7 nm (Fig. 11a) and the average area of these particles is less than 100 nm. These nano graphene oxides have been produced in long time and strong ultrasonication of graphene oxide. Thickness of the NGOs conjugated with two polymers has risen up to 250 nm for Janus nanoparticles (Fig. 11b) and about 30-50 nm for mixed nanoparticles (Fig. 11c). It is reasonable to assume that the mixed nanoparticles consist of NGO layer and monolayer of polymers grafted on both side of NGOs. In this sample, both polymers have uniformly been dispersed on the surface of GO nanoparticles. The significant thickness difference of Janus and mixed nanoparticles shows that the Janus nanoparticles have clustered not only horizontally, but also vertically (Fig. 11d). This would cause the thickness growth up to 250 nm, approximately five times greater than mixed nanoparticles, and is another confirmation for SEM observations.

In addition, fluorescein was also used as a hydrophobic drug model. Fig. 12 shows fluorescence microscopy images of Janus and

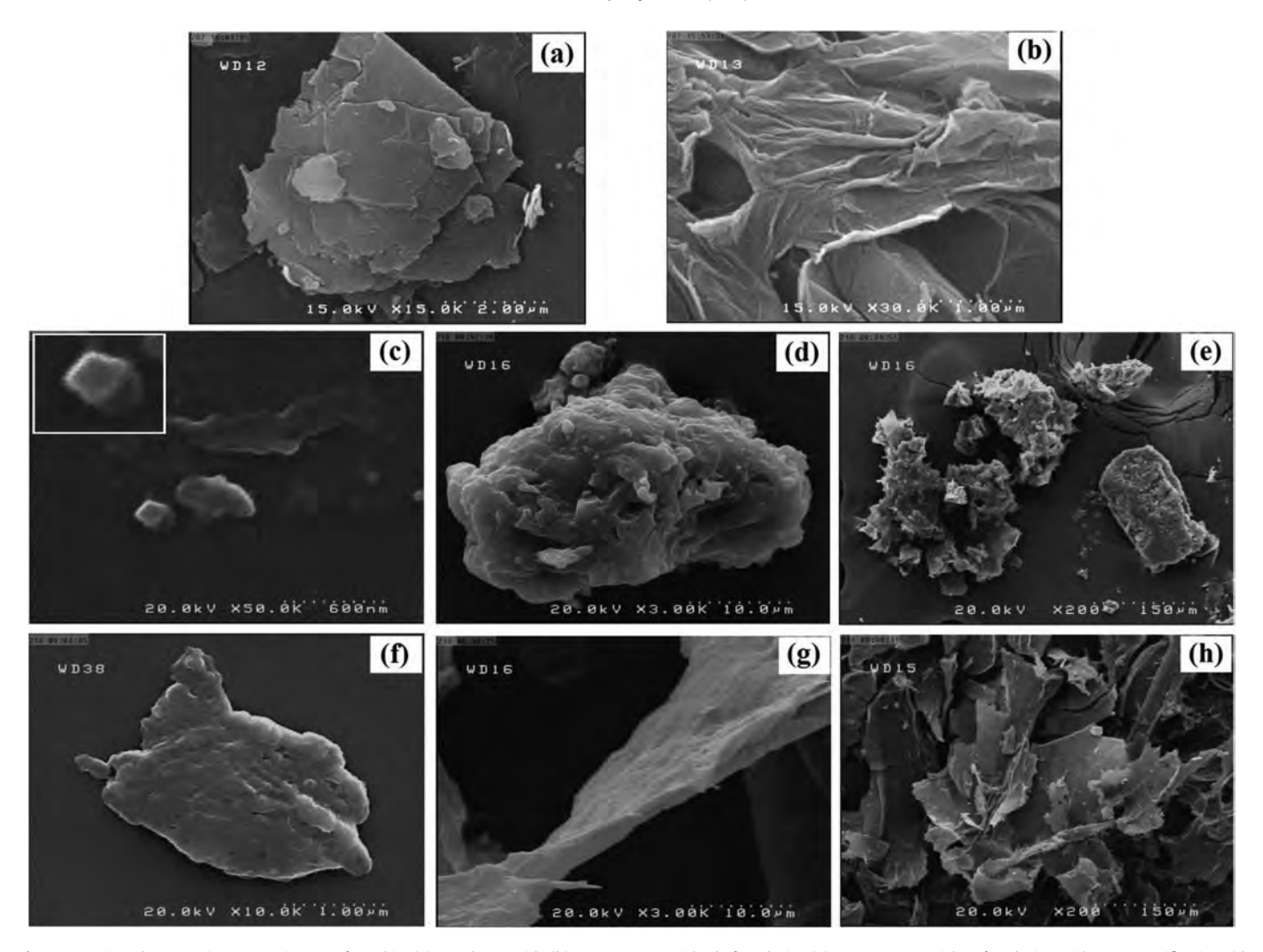


Fig. 9. Scanning electron microscopy pictures of graphite (a), graphene oxide (b), Janus nanoparticles before drying (c), Janus nanoparticles after drying with two magnifications (d and e) mixed nanoparticles before drying (f), mixed nanoparticles after drying with two magnifications (g and h).

mixed nanoparticles with and without fluorescein. The empty Janus and mixed nanoparticles only showed black background (Fig. 12a and b). In the fluorescein-loaded Janus and mixed nanoparticles, the green drugs were observable but, with two different patterns. In Janus nanoparticles (Fig. 12c), the drug molecules were aligned tandem along a straight line. It seems that this rough line was produced by smart assembly of anisotropic nanoparticle and forming an arranged micro-structure. Evidently, this picture shows fluorescein molecules were accumulated much higher in one side of this line (probably in PCL domain) and with more attendance on the borderline between two areas. This means that, hydrophobic drugs with polar substituents tend to locate at the boundaries between two polymers. Accordingly, fluorescein is seen in the whole surface of the mixed nanoparticles (Fig. 12d), since there is an infinite border between the polymers.

3.4. Drug loading of Janus and mixed nanoparticles

To demonstrate the effectiveness of two anti-cancer drugs with different natures *i.e.* natural and synthetic ones, two FDA approved drugs were used: 5-FU and quercetin. 5-FU is a member of pyrimidine analog medications that inhibits the growth of several cancer cell types by blocking the action of thymidylate synthase and thus, stopping the production of DNA. Quercetin is a flavonol

which can be found in many fruits vegetables, leaves, and grains and recently, has been promoted for prevention and treatment of cancer. Following the synthesis of Janus and mixed PCL/Terpolymer nanoparticles, each individual type of nanoparticle was loaded with either quercetin as hydrophobic drug, 5-FU as hydrophilic drug or a combination of above two drugs. The main vision of this project was to deliver two hydrophobic and hydrophilic drugs simultaneously, using only one carrier which has the ability to be loaded with both drugs in order to treat the cancerous cells synergistically. 5-FU is soluble in water, while quercetin is properly soluble in DMF, and does not have adequate solubility in water media. Drug loading was performed through drug trapping method. Feed weight ratio of drug to the nanoparticles was 10:1. EE% and DL were respectively measured from equations (1) and (2). Table 2 contains EE% and DL values for the two nanoparticle types, containing only one or both drugs. The physicochemical properties of the nanoparticles with and without drug(s) were investigated in order to explain their colloidal behavior. First, dynamic light scattering (DLS) data showed that empty Janus and mixed nanoparticles were formed with a mean diameter below 100 nm in PBS solution (Table 2). Increase in the size of nanoparticles after loading with the drug(s) proves the encapsulation of drug(s) in the nanoparticles. The surface charge of empty nanoparticles was positive, the acidic characteristics of phenolic OH groups of quercetin and amidic NH

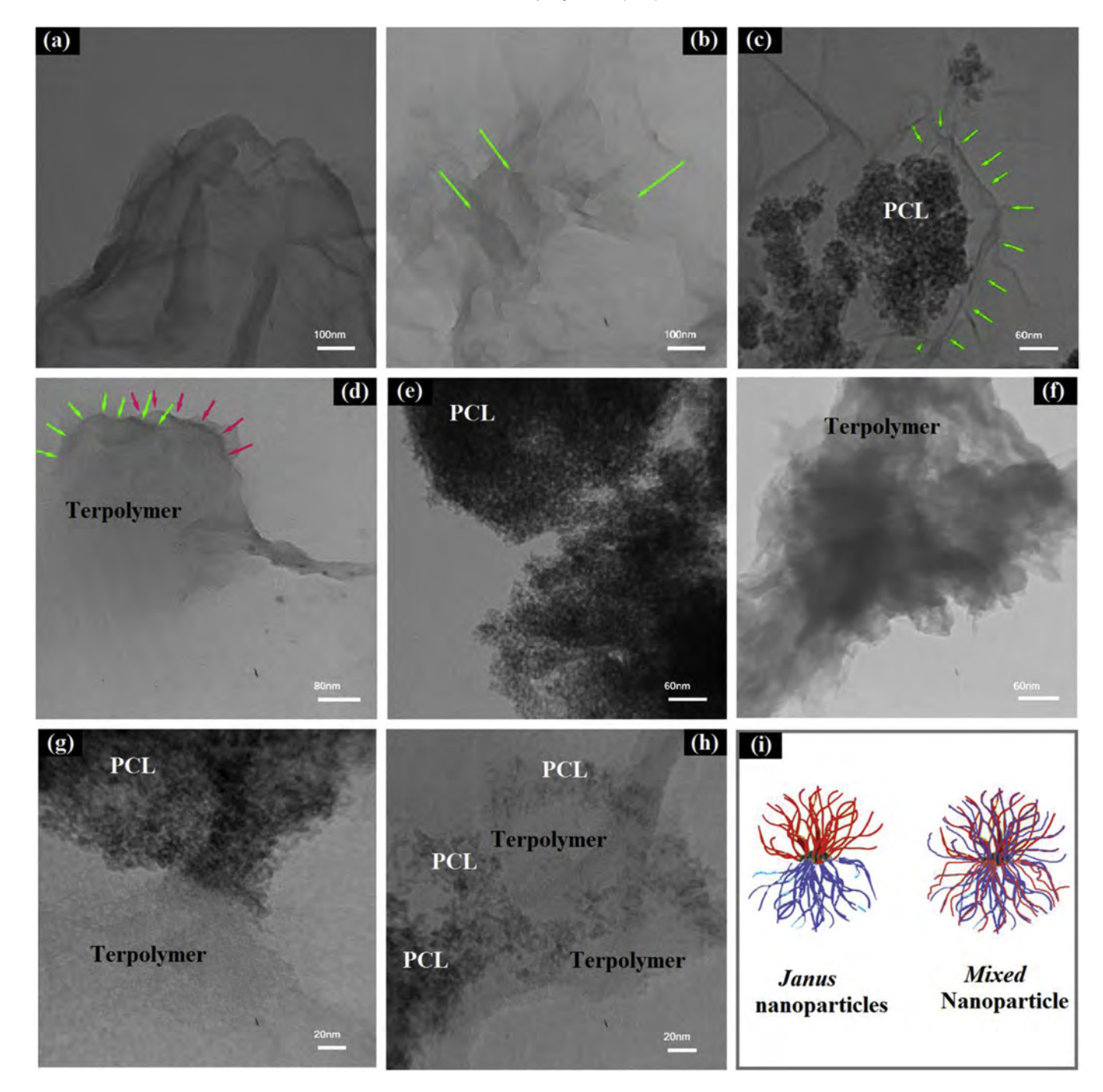


Fig. 10. TEM images of GO (a), NGO (b), *J*-(PCL-NGO) (c), *J*-(NGO-Terpolymer) (d), *m*-(PCL-NGO) (e), *m*-(NGO-Terpolymer) (f), *J*-(PCL-NGO-Terpolymer) (g), *m*-(PCL-NGO-Terpolymer) (h) and Schematic illustration of *J*-(PCL-NGO-Terpolymer) and *m*-(PCL-NGO-Terpolymer) nanoparticles (i).

groups of 5-FU, causing a decrease in zeta potential of the whole system. Consequently, zeta potential values of the drug loaded nanoparticles have decreased, while they are still in a stability range.

Encapsulation efficiency for quercetin in mixed nanoparticles is about 18.5% higher than Janus nanoparticles. Quercetin with two benzene rings, joined by a heterocyclic pyran ring is known to be a hydrophobic drug and its aggregation or dispersion in hydrophobic parts of nanoparticle is expected. The presence of some functional groups with different polarities, such as the hydroxyl groups, makes potentiality for hydrogen bond formation with hydrophilic

parts of the nanoparticle. It seems that due to the dual nature of quercetin, this molecule is positioned to obtain maximum stability *i.e.* at the interface of hydrophobic PCL section and hydrophilic terpolymer. Compared with mixed nanoparticles, less hydrophobic/hydrophilic interfaces can be observed in Janus nanoparticles, since their two sections are located at different sides of the NGO sheet. This separation causes an extremely limited interface in Janus nanoparticles and it will not be inconceivable that Janus nanoparticles show less quercetin loading compared with mixed ones. On the other hand, no notable difference for 5-FU can be observed for mixed and Janus nanoparticles. 5-FU is specifically hydrophilic

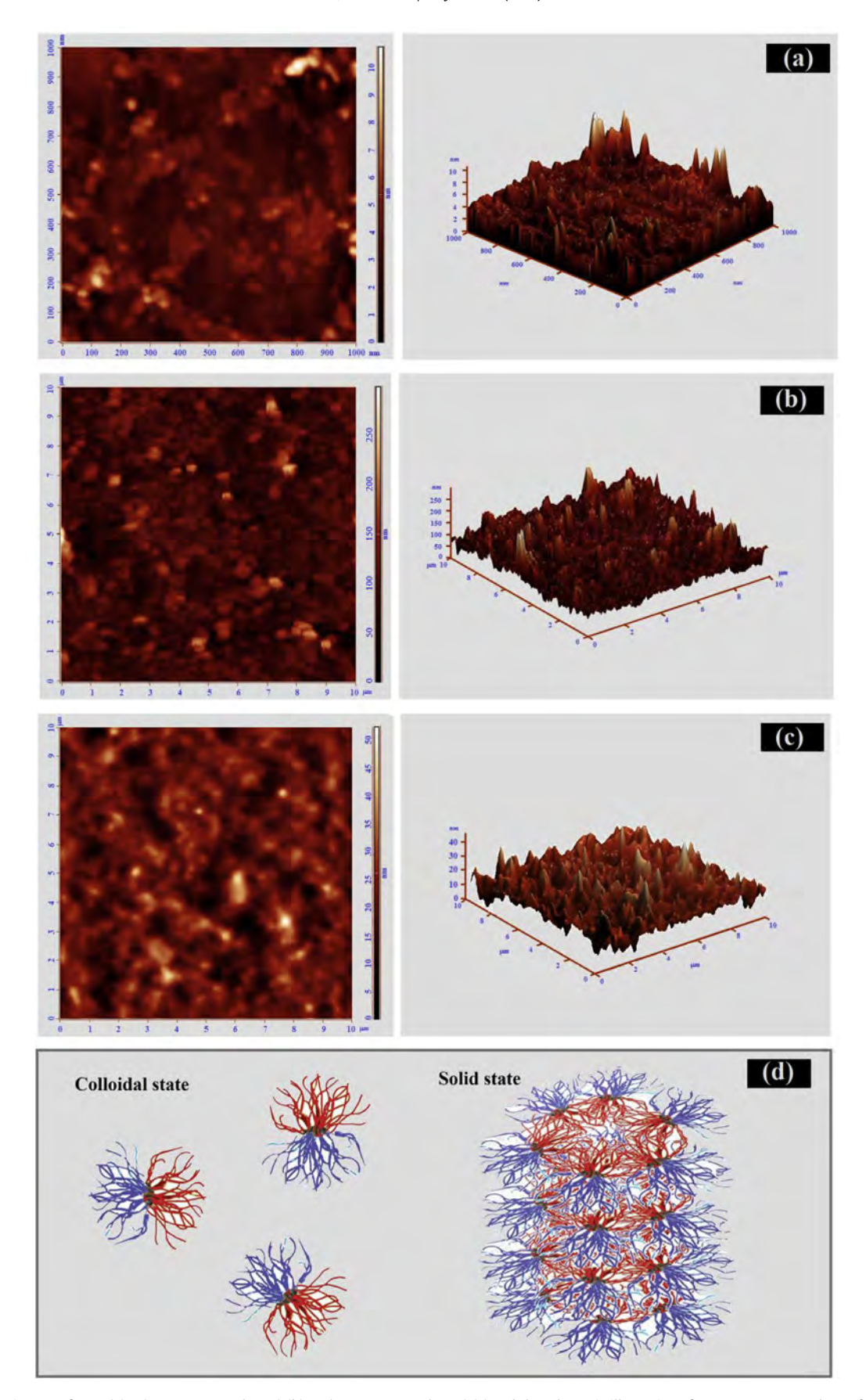


Fig. 11. AFM images of NGO (a), J-(PCL-NGO-Terpolymer) (b), m-(PCL-NGO-Terpolymer) (c) and the schematic illustration of 3D superstructure cluster formation (d).

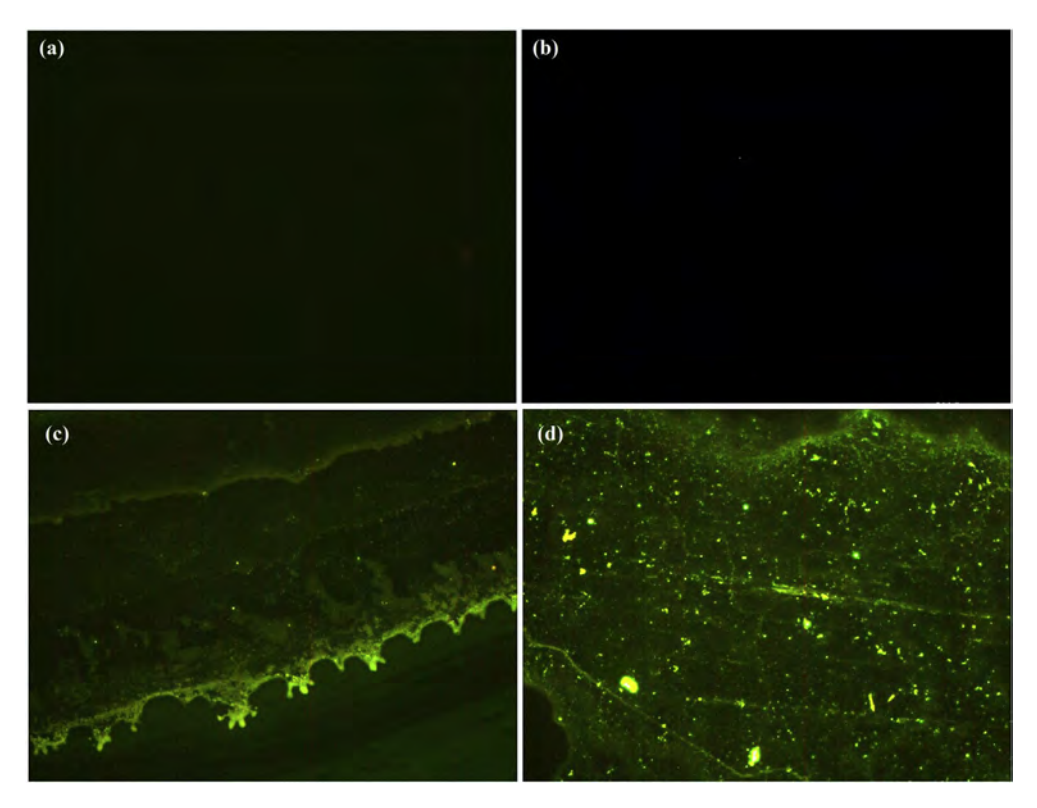


Fig. 12. Fluorescence microscopy images of empty Janus (a) and mixed (b) nanoparticles; fluorescein-loaded Janus (c) and mixed (d) nanoparticles.

 Table 2

 Physical properties of nanoparticles with and without drug(s).

Nanoparticles	Drug ^a	Size (nm)	Size distribution ^b	Zeta potential ^b	Drug loading (%)	Encapsulation efficiency (%)
Janus	_	89	0.25	+19.1	_	_
Mixed	_	74	0.31	+22.5	_	-
Janus	5-FU Quercetin	93	0.22	+17.0	4.46	49.11 _
Janus	5-FU Quercetin	100	0.24	+15.1	_ 7.59	_ 83.5
Janus	5-FU Quercetin	101	0.27	+14.9	3.81 4.84	41.91 53.25
Mixed	5-FU Quercetin	87	0.24	+15.5	3.46 6.52	38.03 71.77

^a Feed weight ratio (drug/polymer = 1: 10).

and is merely loaded in the hydrophilic domains of the nanoparticle. The indifference in 5-FU loading for Janus and mixed nanoparticles seems to be logical hence.

In the next attempt, a combination of two drugs was loaded into each nanoparticle and their results were compared with those of the single drug formulations. When single drug entities are separately loaded in Janus nanoparticles, an increase in EE for both drugs is observed in comparison with simultaneous loading of both drugs. This increase is much higher for quercetin, because of its attraction to both hydrophilic and hydrophobic parts of the nanoparticles and its tendency to be at the interface of two polymers. Since Terpolymer is made up of both hydrophilic and hydrophobic components, it can be a good uptake site for quercetin, especially on its edges. In the absence of 5-FU, quercetin can occupy the cavities of the terpolymer domains that lie in the borderline as well as PCL moieties. On the other hand, 5-FU is completely hydrophilic

and is loaded only in the terpolymer. In the absence of quercetin, terpolymer chains near the hydrophilic/hydrophobic interface are empty and can be occupied by 5-FU molecules, which increase 5-FU loading, although the difference was only 0.65% (Table 2). More interestingly, 5-FU loading in the *mixed* nanoparticles was less than in the *Janus* ones, although this was vice versa for the loading of quercetin.

3.5. In-vitro release studies for Janus and mixed nanoparticles

In-vitro release of quercetin and 5-FU from Janus and mixed nanoparticles was carried out in PBS at 37 and 40 °C and pH value of 7.4 (Fig. 13). Release rate of 5-FU is higher than quercetin in Janus nanoparticle in mono drug loading procedure (Fig. 13a and b), which is due to the higher solubility of 5-FU in PBS media. Furthermore, thermo-sensitive polymers are potent to release the

b In aqueous solution at a concentration of 0.1 mg/mL at 25 °C.

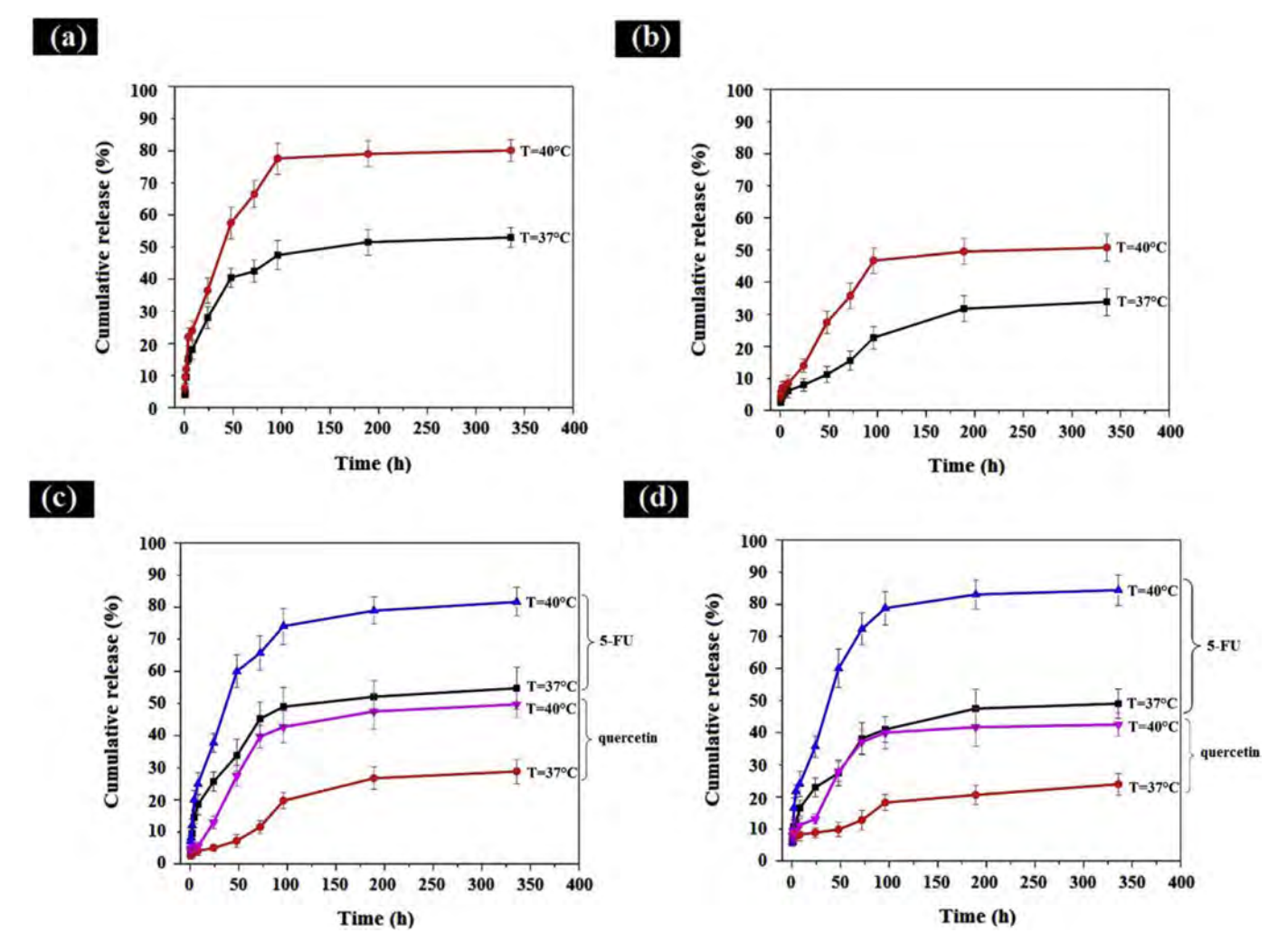


Fig. 13. In-vitro release of 5-FU (a), Quercetin (b), dual drugs from J-(PCL-NGO-Terpolymer) (c) and dual drugs from m-(PCL-NGO-Terpolymer) (d).

loaded cargo specifically inside cancerous cells because of higher temperature of these cells than normal cells. To evaluate the thermal sensitivity of these nanoparticles, their drug release profiles were also measured at above their transition temperature (i.e. $40\,^{\circ}\text{C}$). As expected, release curves show that release rate at $40\,^{\circ}\text{C}$ is higher than 37 °C. At high temperature and due to the existence of amide groups, terpolymer forms intermolecular hydrogen bonds which dissociate at lower temperature through the so-called "zipper effect" [29].

The effect of nanoparticles architecture on the *in-vitro* dual drug release profile from each nanoparticle is shown in Fig. 13c and d. Compared with quercetin, 5-FU release rate from both nanoparticles is higher, just like the samples with single drug. The thermal-responsive behavior of two nanoparticles with dual drugs is also similar to the one obtained from one drug. The results indicate that 5-FU release is more dependent on temperature than quercetin, because it is mainly loaded in terpolymer, while quercetin is loaded in the polymer interface and also has interactions with PCL chains.

3.6. Cytotoxicity tests

This study will clarify which one of the Janus or mixed arrangements are suitable for *in-vivo* and *in-vitro* applications. We evaluated biocompatibility of the particles using MTT assay on C6

and OLN-93 cells. Fig. 14 shows viability of the incubated cells with 5-FU, quercetin, 5-FU/quercetin, empty nanoparticles, and drug loaded nanoparticles at different concentrations for 24 h at 37 and 40 °C. Free Janus particles compared to free mixed ones have low toxicity, especially at higher concentrations and interestingly, would not show distinctive increase at higher temperature. Quercetin, 5-FU or even combined drugs did not suppress cell proliferation at two temperatures, indicating that the individual or combined drugs were not more toxic at higher temperature. As illustrated, quercetin-loaded Janus nanoparticles are more toxic at both temperatures compared to its free drug. This is due to the significant increase in solubility of the nanoparticulated formulation of quercetin in the aqueous media in comparison with the free quercetin suspension, or in other words, indicates the improved bioavailability of the nano-drug. Our results show that the Janus nanoparticles containing 5-FU have low cytotoxicity that may commonly be related to the interactions between drug and terpolymer. In the case of the Janus nanoparticles which contain two drugs at 37 °C, they are less toxic than free combined drugs. But at 40 °C, they are notably more toxic than free drugs at the same situations, specifically at higher concentrations (i.e. 100 and 500 µM). We found that, synergetic effect of combined drugs in contact with cancerous cells at higher temperature is acceptable and can be considered as a favorable result.

We performed the inhibitory effect of different nanoparticles on

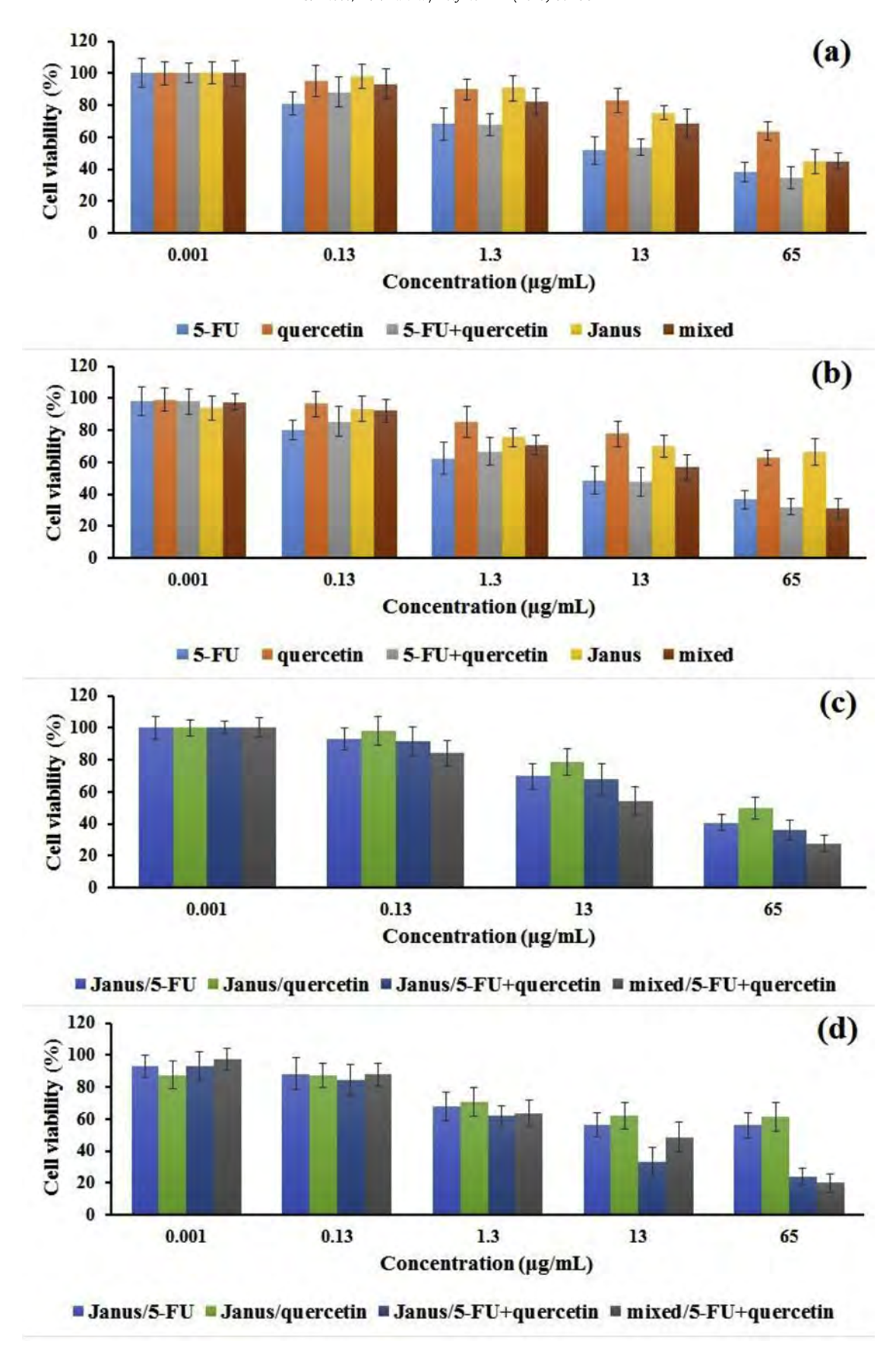


Fig. 14. The cytotoxicity of pure drugs, Janus and mixed nanoparticles without drug at $37 \,^{\circ}\text{C}$ (a) and $40 \,^{\circ}\text{C}$ (b), single and dual drug loaded Janus nanoparticles and dual drug loaded mixed nanoparticles at $37 \,^{\circ}\text{C}$ (c) and $40 \,^{\circ}\text{C}$ (d) on C6 cells after $24 \,^{\circ}\text{h}$ incubation.

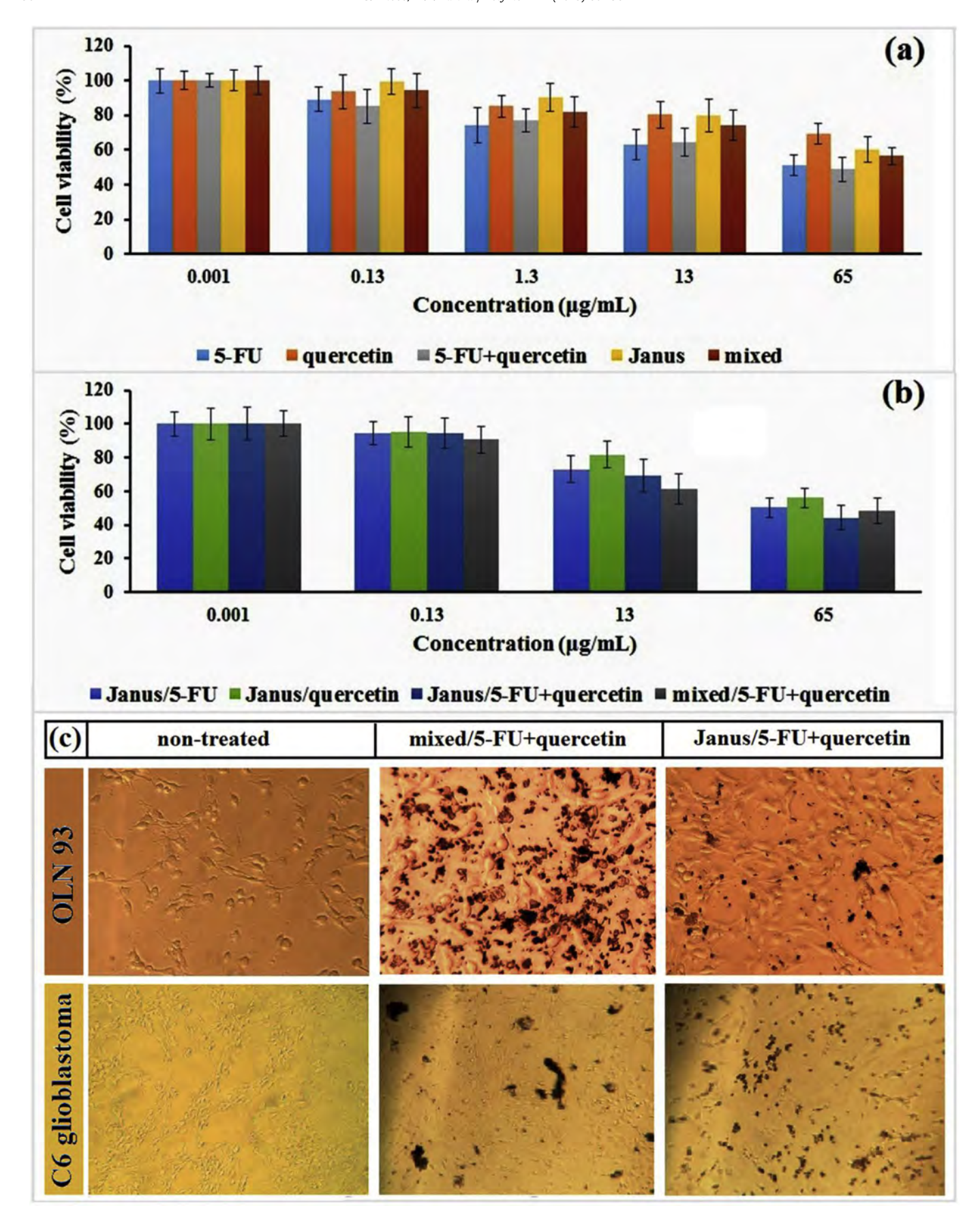


Fig. 15. The cytotoxicity of pure drugs, *Janus* and *mixed* nanoparticles without drug (a), as well as single and dual drug loaded *Janus* nanoparticles and dual drug loaded *mixed* nanoparticles (b) on OLN 93 cells at 37 °C; and representative optical microscopy images of normal and cancerous brain cells without nanoparticles (non-treated), with *mixed*- and *Janus*-nanoparticles (c).

cell proliferation of OLN-93 as normal cell, similar to those for C6 cells. Fig. 15 (a and b) shows the viability of OLN-93 cells incubated with 5-FU, quercetin, 5-FU/quercetin, empty nanoparticles, and drug loaded nanoparticles at different concentrations for 24 h at 37 °C. When the concentration of nanoparticles is increased, cell viability of OLN-93 is decreased. Results show that both Ianus and mixed nanoparticles can inhibit the proliferation of normal cells. However, the inhibitions of cancer cell proliferation are much greater than those of normal cell proliferation. It was also found that the inhibitory effect of dual drugs-loaded nanoparticles on normal cells was dependent on the morphology of nanoparticles and highest degree of inhibition was observed with mixed nanoparticles. To examine the quality of nanoparticles internalization into the cell lineages, we used optical microscopy to image the behavior of various nanoparticles with brain normal cell at 37 °C and with brain cancer cell at 40 °C (i.e. under approximately similar temperature of normal and cancerous cells). As shown in Fig. 15c at low temperature, the greater number of internalization in treated normal cells was observed for mixed nanoparticle. Under similar condition, a reverse trend was found for Janus nanoparticles. This difference is returns to the formation of large aggregates of Janus nanoparticles on the cell surface. Interestingly, at elevated temperature the interparticle interactions between Janus nanoparticles were broken and consequently, the produced individual nanoparticles have got the potentiality to internalize into tumor cell more quickly. Optical microscopy image of cancer cells with mixed nanoparticles demonstrates the accumulation of these nanoparticles on the cell surface. These results show that the observed difference in the degree of inhibition of cancer cells at 40 °C and normal cells at 37 °C by two types of nanoparticles should be attributed to their specific morphologies.

4. Conclusion

In this work, we have utilized two methods to prepare polymer modified graphene oxide nanoparticles with mixed and Janus morphologies and used these vehicles for dual drug delivery system. Accordingly, symmetrical alkynyl-GO was synthesized via a two-step method as 2D nanomaterial that has remarkable stabilization effect for the oil-in-water interface. A thermo-responsive NIPAAm-based nanocarrier system was developed as hydrophilic domain and biocompatible PCL as hydrophobic one. 2D Janus nanodisc was prepared from the click reaction of azidated polymers with NGO alkynyl groups through Pickering emulsion of oil in water. The assembled Janus nanostructures not only provide the thermosensitivity and improved biocompatibility, but also give the opportunity to facilitate the release of drug after excitation by nearinfrared light. 5-FU and quercetin drugs were loaded on the prepared Janus and mixed nanoparticles. On the basis of hydro-affinity of these drugs, they were loaded on different parts of the nanoparticles. Quercetin was loaded on the barrier line of two different polymers and 5-FU was loaded on the terpolymer. Since the total barrier line length in Janus nanoparticles is shorter than mixed nanoparticles, the loading amount of quercetin is higher in the mixed nanoparticle. Drug release and toxicity tests at two different temperatures demonstrate that nanoparticles are sensitive to temperature changes and would release more drugs at 40 °C compared with the drug release at 37 °C.

Acknowledgements

Sincere thanks are given to Prof S. Khoei and his group in Iran University of Medical Sciences (IUMS), Tehran, Iran, for generously supporting our cell viability assay experiments and Dr. Bahman Zeinali in University of Tehran, Tehran, Iran, for allowing access to

Zeiss Axioplan 2 fluorescence microscope.

References

- K.I. David, L.R. Jaidev, S. Sethuraman, U.M. Krishnan, Dual drug loaded chitosan nanoparticles—sugar-coated arsenal against pancreatic cancer, Colloids Surf. B 135 (2015) 689–698.
- [2] P. Parhi, C. Mohanty, S.K. Sahoo, Nanotechnology-based combinational drug delivery: an emerging approach for cancer therapy, Drug Discov. Today 17 (2012) 1044–1052.
- [3] J.N. Lockhart, D.M. Stevens, D.B. Beezer, A. Kravitz, E. Harth, Dual drug delivery of tamoxifen and quercetin: regulated metabolism for anticancer treatment with nanosponges, J. Contr. Release 220 (2015) 751–757.
- [4] A. Kundu, S. Nandi, P. Das, A.K. Nandi, Fluorescent graphene oxide via polymer grafting: an efficient nanocarrier for both hydrophilic and hydrophobic drugs, ACS Appl. Mater. Interfaces 7 (2015) 3512–3523.
- [5] W. Scarano, P. de Souza, M.H. Stenzel, Dual-drug delivery of curcumin and platinum drugs in polymeric micelles enhances the synergistic effects: a double act for the treatment of multidrug-resistant cancer, Biomater. Sci. 3 (2015) 163–174.
- [6] T. Kubota, Y. Uemura, M. Kobayashi, H. Taguchi, Combined effects of resveratrol and paclitaxel on lung cancer cells, Anticancer Res. 23 (2002) 4039–4046.
- [7] A. Mohan, S. Narayanan, S. Sethuraman, U. Maheswari Krishnan, Combinations of plant polyphenols & anti-cancer molecules: a novel treatment strategy for cancer chemotherapy, Anti Canc. Agents Med. Chem. 13 (2013) 281–295
- [8] C. Kaewsaneha, P. Tangboriboonrat, D. Polpanich, M. Eissa, A. Elaissari, Janus colloidal particles: preparation, properties, and biomedical applications, ACS Appl. Mater. Interfaces 5 (2013) 1857–1869.
- [9] Y.-S. Wang, D. Shao, L. Zhang, X.-L. Zhang, J. Li, J. Feng, H. Xia, Q.-S. Huo, W.-F. Dong, H.-B. Sun, Gold nanorods-silica Janus nanoparticles for theranostics, Appl. Phys. Lett. 106 (2015) 173705.
- [10] L.-T.-C. Tran, S. Lesieur, V. Faivre, Janus nanoparticles: materials, preparation and recent advances in drug delivery, Expet Opin. Drug Deliv. 11 (2014) 1061–1074.
- [11] W. He, J. Frueh, Z. Wu, Q. He, Leucocyte membrane-coated janus microcapsules for enhanced photothermal cancer treatment, Langmuir 32 (2016) 3637–3644.
- [12] A. Walther, A.H. Müller, Janus particles, Soft Matter 4 (2008) 663-668.
- [13] K.-C. Mei, N. Rubio, P.M. Costa, H. Kafa, V. Abbate, F. Festy, S.S. Bansal, R.C. Hider, K.T. Al-Jamal, Synthesis of double-clickable functionalised graphene oxide for biological applications, Chem. Commun. 51 (2015) 14981–14984.
- [14] S.A. Sydlik, S. Jhunjhunwala, M.J. Webber, D.G. Anderson, R. Langer, In vivo compatibility of graphene oxide with differing oxidation states, ACS Nano 9 (2015) 3866–3874.
- [15] Y. Yang, L. Zhang, X. Ji, L. Zhang, H. Wang, H. Zhao, Preparation of Janus graphene oxide (GO) nanosheets based on electrostatic assembly of GO nanosheets and polystyrene microspheres, Macromol. Rapid Commun. 37 (2016) 1520–1526.
- [16] J. Yun, F.A. Khan, S. Baik, Janus graphene oxide sponges for high-purity fast separation of both water-in-oil and oil-in-water emulsions, ACS Appl. Mater. Interfaces 9 (2017) 16694–16703.
- [17] H. Wu, W. Yi, Z. Chen, H. Wang, Q. Du, Janus graphene oxide nanosheets prepared via Pickering emulsion template, Carbon 93 (2015) 473–483.
- [18] D. Luo, F. Wang, M.K. Alam, F. Yu, I.K. Mishra, J. Bao, R.C. Willson, Z. Ren, Colloidal stability of graphene-based amphiphilic Janus nanosheet fluid, Chem. Mater. 29 (2017) 3454–3460.
- [19] J. Orozco, L.A. Mercante, R. Pol, A. Merkoçi, Graphene-based Janus micromotors for the dynamic removal of pollutants, J. Mater. Chem. 4 (2016) 3371–3378.
- [20] H.J. Ryu, S.S. Mahapatra, S.K. Yadav, J.W. Cho, Synthesis of click-coupled graphene sheet with chitosan: effective exfoliation and enhanced properties of their nanocomposites, Eur. Polym. J. 49 (2013) 2627–2634.
- [21] Z. Shen, W. Wei, Y. Zhao, G. Ma, T. Dobashi, Y. Maki, Z. Su, J. Wan, Thermosensitive polymer-conjugated albumin nanospheres as thermal targeting anticancer drug carrier, Eur. J. Pharmaceut. Sci. 35 (2008) 271–282.
- [22] D.C. Marcano, D.V. Kosynkin, J.M. Berlin, A. Sinitskii, Z. Sun, A. Slesarev, L.B. Alemany, W. Lu, J.M. Tour, Improved synthesis of graphene oxide, ACS Nano 4 (2010) 4806–4814.
- [23] W. Li, X. Liu, G. Qian, J. Deng, Immobilization of optically active helical polyacetylene-derived nanoparticles on graphene oxide by chemical bonds and their use in enantioselective crystallization, Chem. Mater. 26 (2014) 1948–1956
- [24] L. Xu, L. Che, J. Zheng, G. Huang, X. Wu, P. Chen, L. Zhang, Q. Hu, Synthesis and thermal degradation property study of N-vinylpyrrolidone and acrylamide copolymer, RSC Adv. 4 (2014) 33269–33278.
- [25] J. Kim, L.J. Cote, F. Kim, W. Yuan, K.R. Shull, J. Huang, Graphene oxide sheets at interfaces, J. Am. Chem. Soc. 132 (2010) 8180–8186.
- [26] T.M. McCoy, M.J. Pottage, R.F. Tabor, Graphene oxide-stabilized oil-in-water emulsions: pH-controlled dispersion and flocculation, J. Phys. Chem. C 118 (2014) 4529–4535.
- [27] S.B. Munteanu, C. Vasile, Spectral and thermal characterization of styrene-

- butadiene copolymers with different architectures, J. Optoelectron. Adv. Mater. 7 (2005) 3135–3148.

 [28] L. Shao, J.L. Lutkenhaus, Thermochemical properties of free-standing electrostatic layer-by-layer assemblies containing poly (allylamine hydrochloride)
- and poly (acrylic acid), Soft Matter 6 (2010) 3363—3369.

 [29] H. Dai, Q. Chen, H. Qin, Y. Guan, D. Shen, Y. Hua, Y. Tang, J. Xu, A temperature-responsive copolymer hydrogel in controlled drug delivery, Macromolecules 39 (2006) 6584—6589.